Redox Biology 59 (2023) 102588

Contents lists available at ScienceDirect

Redox Biology

journal homepage: www.elsevier.com/locate/redox

Lpp of *Escherichia coli* K1 inhibits host ROS production to counteract neutrophil-mediated elimination

Xue-Wei Zhang [a], Ming-Xin An [a], Zeng-Kang Huang [a], Lan Ma [a], Dan Zhao [a,b], Zhao Yang [a], Jun-Xiu Shi [a], Dong-Xin Liu [a], Qiang Li [c], An-Hua Wu [b], Yu-Hua Chen [a], Wei-Dong Zhao [a,*]

[a] *Department of Developmental Cell Biology, Key Laboratory of Cell Biology, Ministry of Public Health, and Key Laboratory of Medical Cell Biology, Ministry of Education, China Medical University, 77 Puhe Road, Shenbei New District, Shenyang, 110122, China*
[b] *Department of Neurosurgery, the First Hospital of China Medical University, 155 Nanjing Street, Heping District, Shenyang, 110001, China*
[c] *Department of Laboratory Medicine, Shengjing Hospital of China Medical University, 16 Puhe Road, Shenbei New District, Shenyang, 110134, China*

ARTICLE INFO

Keywords:
Escherichia coli K1
Bacterial meningitis
Neutrophil
Lpp
ROS
Bacteremia
FliC

ABSTRACT

Escherichia coli (*E. coli*) is the most common Gram-negative bacterial organism causing neonatal meningitis. The pathogenesis of *E. coli* meningitis, especially how *E. coli* escape the host immune defenses, remains to be clarified. Here we show that deletion of bacterial *Lpp* encoding lipoprotein significantly reduces the pathogenicity of *E. coli* K1 to induce high-degree of bacteremia necessary for meningitis. The *Lpp*-deleted *E. coli* K1 is found to be susceptible to the intracellular bactericidal activity of neutrophils, without affecting the release of neutrophil extracellular traps. The production of reactive oxygen species (ROS), representing the primary antimicrobial mechanism in neutrophils, is significantly increased in response to *Lpp*-deleted *E. coli*. We find this enhanced ROS response is associated with the membrane translocation of NADPH oxidase $p47^{phox}$ and $p67^{phox}$ in neutrophils. Then we constructed $p47^{phox}$ knockout mice and we found the incidence of bacteremia and meningitis in neonatal mice induced by *Lpp*-deleted *E. coli* is significantly recovered by $p47^{phox}$ knockout. Proteomic profile analysis show that *Lpp* deficiency induces upregulation of flagellar protein FliC in *E. coli*. We further demonstrate that FliC is required for the ROS induction in neutrophils by *Lpp*-deleted *E. coli*. Taken together, these data uncover the novel role of *Lpp* in facilitating intracellular survival of *E. coli* K1 within neutrophils. It can be inferred that Lpp of *E. coli* K1 is able to suppress FliC expression to restrain the activation of NADPH oxidase in neutrophils resulting in diminished bactericidal activity, thus protecting *E. coli* K1 from the elimination by neutrophils.

1. Introduction

Escherichia coli (*E. coli*) is the most common Gram-negative bacterial organism causing neonatal meningitis [1–3]. Despite the introduction of antibiotics and advances in intensive care, neonatal *E. coli* meningitis continues to be an important cause of mortality and morbidity [4] and a major contributing factor is the incomplete knowledge of the pathogenesis of *E. coli* meningitis.

At the initial stage of bacterial infection, neutrophils are the first immune cells recruited toward the site of infection, providing the early protective defense against the invading bacteria [5]. During *E. coli* meningitis, numerous circulating neutrophils are actively recruited and crossed the blood-brain barrier (BBB) to counteract the bacteria [6]. The significantly increased number of neutrophils in the cerebrospinal fluid (CSF) of individuals with *E. coli* meningitis results in the cloudy appearance of CSF, which is the characteristic feature of bacterial meningitis [7].

The circulating neutrophils are recruited to the infectious sites in response to pathogen invasion. The pathogens are captured and internalized into neutrophils by phagocytosis forming membrane-enclosed phagosomes [5]. Within phagosomes, the engulfed pathogens are exposed to various microbicidal peptides, destructive enzymes and reactive oxygen species (ROS) causing significant degradation [5,8]. In addition to phagocytosis, recent studies revealed that neutrophil extracellular traps (NETs) are employed by neutrophils to entrap and attack the pathogens in the extracellular space [9].

The generation of ROS, such as superoxide anion ($O2^-$), hydrogen peroxide (H_2O_2) and hydroxyl radical ($OH^•$), is regarded as the

* Corresponding author.
E-mail address: wdzhao@cmu.edu.cn (W.-D. Zhao).

https://doi.org/10.1016/j.redox.2022.102588
Received 20 November 2022; Received in revised form 15 December 2022; Accepted 22 December 2022
Available online 26 December 2022

predominant antimicrobial mechanism of neutrophils [8]. These ROS can diffuse across the membrane of the bacteria and damage bacterial nucleic acids, proteins and lipids, causing restriction of bacterial growth [10]. By contrast, the bacteria develop a series of strategies to resist the damages by ROS. Some of the bacteria, such as *Salmonella typhimurium* [11], *Listeria monocytogenes* [12], and *Pseudomonas aeruginosa* [13], can interfere with the activity of ROS generation machinery in neutrophils. Unraveling the regulatory mechanism of ROS production in neutrophils in the context of pathogen-host interaction may lead to new strategies for the treatment of bacterial infection.

Lipoprotein (Lpp) belongs to a large family of bacterial envelope proteins that are attached to the outer membrane or cytoplasmic membrane of Gram-negative bacteria by a lipid moiety [14]. The role of lipoproteins in maintaining bacterial envelope integrity and regulating the width of the periplasmic space was reported in *Salmonella enterica* [15] and the non-pathogenic *E. coli* K-12 [16]. From the host perspective, the involvement of Lpp in host inflammatory responses has been implicated in previous studies. Lpp of *Salmonella enterica* serovar Typhimurium may induce the release of proinflammatory cytokines such as tumor necrosis factor-α and interleukin (IL)-8 in macrophage and epithelial cell lines [17]. The purified lipoprotein, Lip, of *Neisseria gonorrhoeae* is capable of inducing IL-8 and IL-6 production in

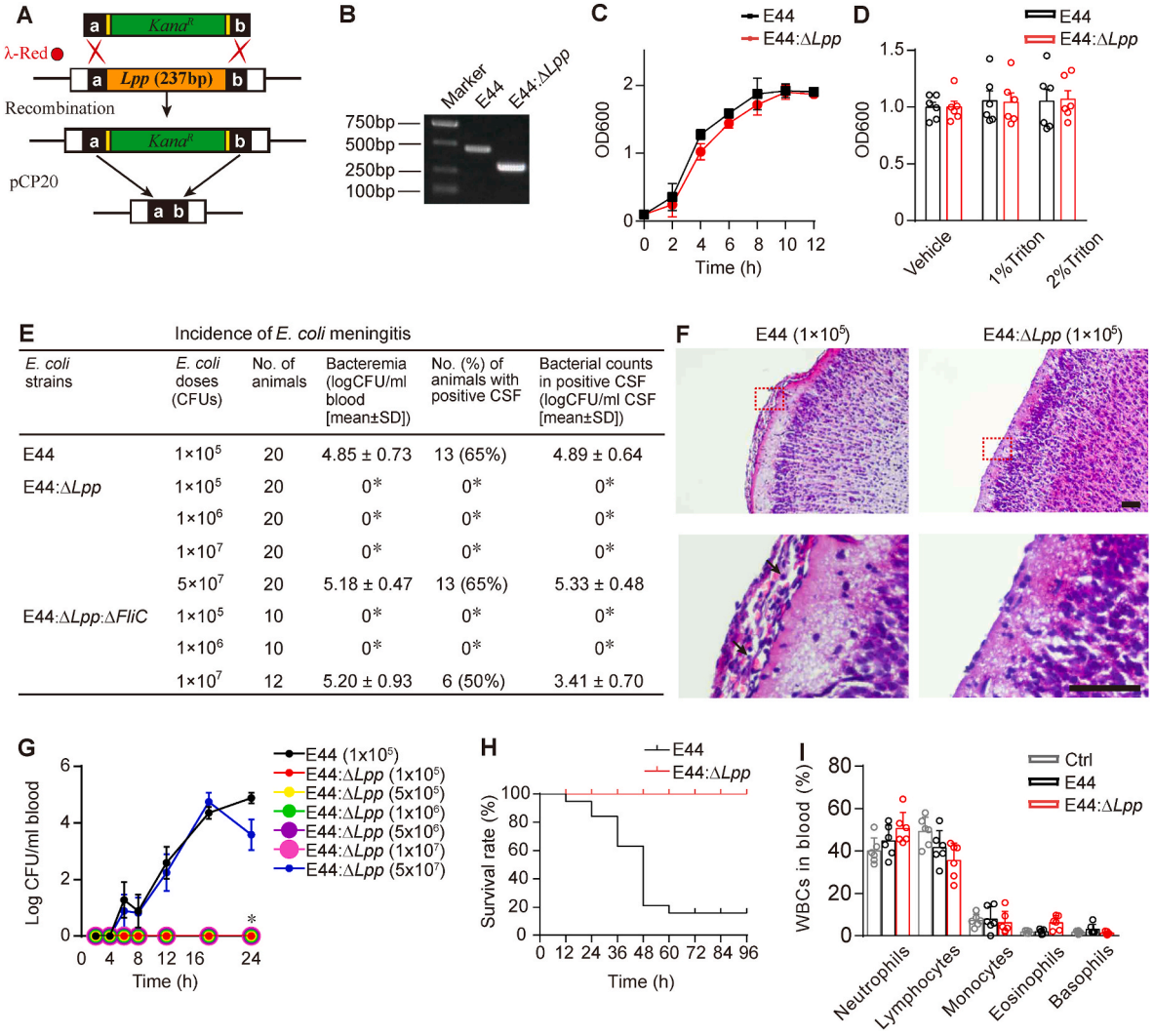

E

Incidence of *E. coli* meningitis

E. coli strains	*E. coli* doses (CFUs)	No. of animals	Bacteremia (logCFU/ml blood [mean±SD])	No. (%) of animals with positive CSF	Bacterial counts in positive CSF (logCFU/ml CSF [mean±SD])
E44	1×10^5	20	4.85 ± 0.73	13 (65%)	4.89 ± 0.64
E44:Δ*Lpp*	1×10^5	20	0*	0*	0*
	1×10^6	20	0*	0*	0*
	1×10^7	20	0*	0*	0*
	5×10^7	20	5.18 ± 0.47	13 (65%)	5.33 ± 0.48
E44:Δ*Lpp*:Δ*FliC*	1×10^5	10	0*	0*	0*
	1×10^6	10	0*	0*	0*
	1×10^7	12	5.20 ± 0.93	6 (50%)	3.41 ± 0.70

Fig. 1. Deletion of *Lpp* gene in *E. coli* K1 reduced the incidence of bacteremia and meningitis.
(A) The strategy of deletion of *Lpp* gene in E44 strain. *Lpp* gene in E44 genome was replaced by the DNA fragment containing kanamycin resistance gene ($Kana^R$) by homologous recombination. Then the resistance gene was removed by the helper plasmid pCP20 to obtain the gene with *Lpp* deletion. (B) The DNA was extracted from the *E. coli* strains and PCR was performed followed by gel electrophoresis. (C) The growth curves of *E. coli* strains in LB broth at 37 °C, 225 rpm. The optical density at 600 nm (OD 600) was measured at indicated times ($n = 6$). (D) The bacteria were cultured until the OD 600 reached to 0.5, then Triton X-100 was added to the indicated concentrations followed by further incubation for 3 h at 37 °C, 225 rpm. Then the OD 600 was recorded ($n = 6$); (E) The 5-day-old neonatal rats were inoculated with indicated dose of *E. coli* subcutaneously. The blood from tail vein and CSF were collected 18 h post-infection, to assess the bacteremia and the occurrence of meningitis, respectively. 2 μl blood or CSF samples were serially diluted and plated on the LB agar plate to count the CFUs following overnight culture at 37 °C. The rate of meningitis occurrence was calculated by dividing the number of rats with positive CSF culture by the total number of rats. (F) The brain sections of neonatal rats inoculated with *E. coli* 18 h post-infection were prepared for hematoxylin and eosin (H&E) staining. The zoom-in view (bottom panel) showing the meningeal thickening and neutrophils infiltration (arrows) were provided. Scale, 100 μm. The images shown are representative of six independent experiments. (G) The 5-day-old neonatal rats were inoculated with *E. coli* subcutaneously. The blood were collected from the tail vein at indicated times post-infection, and the serial diluted samples were plated on LB agar plates. The CFUs were counted following incubation at 37 °C overnight. The results were presented as *mean* ± *SEM* ($n = 8$). *, $P < 0.05$. (H) The survival curves of 5-day-old rats injected with 1×10^5 CFU *E. coli* subcutaneously ($n = 20$ for each group). The numbers of animals alive was recorded every 12 h. (I) The 5-day-old rats were injected with 1×10^5 CFU *E. coli* subcutaneously. Then the blood were collected 18 h post-infection and the percentages of WBCs were measured (n = 6 for each group).

endocervical epithelial cell line [18]. Notably, lipoprotein not only enhances the immune responses but can also suppress immune reactions under certain conditions. For example, deletion of Braun lipoprotein in *Yersinia Pestis* elicits higher levels of cytokine production in murine T cells and macrophages [19]. Thus, the exact mechanism of bacterial Lpp during infection represents a topic worth further investigation for a number of pathogens.

E. coli with K1 capsule is the most common cause of neonatal *E. coli* meningitis [20]. The functional role of bacterial lipoproteins during *E. coli* K1-host interaction remained largely unknown. In this study, using an *Lpp*-deleted *E. coli* K1 strain, we found that *Lpp* deficiency significantly reduced the meningitis rate in neonatal rodents infected with *E. coli* K1, due to the accelerated clearance of bacteria by neutrophils to inhibit the progression of bacteremia necessary for meningitis. Further results demonstrated that Lpp suppressed the expression of flagella protein FliC to restrain the activation of NADPH oxidases in neutrophils resulting in impaired oxidative burst and bactericidal activity, thus protecting *E. coli* K1 from the elimination by neutrophils.

2. Results

2.1. Deletion of Lpp significantly attenuates the pathogenicity of E. coli K1

To study the role of *Lpp* gene in *E. coli* K1, deletion of *Lpp* was performed with λ-Red recombination system in wild-type *E. coli* K1 strain (E44). The chimeric PCR primers flanking *E. coli* K1 *Lpp* gene were designed, and a DNA fragment containing homologous arm of *Lpp* and kanamycin resistance gene were obtained by PCR. Then the fragment was transformed to E44 strain to replace the *Lpp* gene by homologous recombination. The strain containing the fragment was then transformed with pCP20 construct encoding the flippase to remove the kanamycin resistance cassette, generating the *Lpp*-deficient strain E44:Δ*Lpp* (Fig. 1A). The knockout of *Lpp* gene was verified by colony PCR (Fig. 1B) followed by DNA sequencing. The bacterial growth curves, measured by the absorbance of OD 600 nm, showed that the growth rates of wild-type E44 and mutant E44:Δ*Lpp* strains were similar (Fig. 1C). To test whether *Lpp* deficiency affected the membrane integrity of *E. coli*, detergent Triton X-100 (1–2%) was added to the bacterial culture followed by assessment of the bacterial growth. The results showed that deletion of *Lpp* had little effect on the membrane permeability of *E. coli* K1 (Fig. 1D).

The pathogenicity of E44:Δ*Lpp* was then analyzed in the neonatal model of meningitis with 5-day-old rats. The neonatal rats were inoculated with *E. coli* by subcutaneous injection, then the blood and cerebrospinal fluid (CSF) specimens were collected at 18 h post-infection and cultured on the LB agar plate to assess bacteremia and meningitis, respectively. The results showed that, after the inoculation with 1×10^5 E44, the quantity of *E. coli* in the blood was 4.85 ± 0.73 (log CFU/ml of blood), causing a 65% incidence of meningitis defined as positive CSF culture (Fig. 1E). Interestingly, we found that none of the neonatal rats inoculated with 1×10^5 to 1×10^7 E44:Δ*Lpp* exhibited detectable levels of bacteremia and meningitis among the 20 rats tested ($P < 0.05$, χ^2 test, Fig. 1E) (the limit of detection is 3.7 log CFU/ml for blood and CSF samples). When the inoculation of E44:Δ*Lpp* was increased to 5×10^7, the *E. coli* concentration in the blood was elevated from zero to 5.18 ± 0.47 logCFU/ml, accompanied with an increased rate of meningitis incidence to 65% (Fig. 1E). Brain sections of the infected neonatal rats were examined by hematoxylin and eosin (H&E) staining. Thickened meninges with neutrophil infiltration was observed in the rats inoculated with 1×10^5 E44, whereas no discernible histopathology was observed in the meninges of the rats infected with 1×10^5 E44:Δ*Lpp* (Fig. 1F). Then we examined the dynamics of bacteremia. The results showed that, with the inoculation of 1×10^5 *E. coli*, the E44-induced bacteremia occurred early at 6 h post-inoculation and the quantity of bacteria increased with time (Fig. 1G). In contrast, in the case of E44:Δ*Lpp*, the blood culture remained negative during the whole 24-h period after inoculation with 1×10^5 to 1×10^7 *E. coli* (Fig. 1G). Only 500-fold greater inoculation with 5×10^7 CFU E44:Δ*Lpp* can induce bacteremia in neonatal rats to the similar levels as that inoculated with 1×10^5 CFU wild-type E44 (Fig. 1G). The results of survival curves indicated that 80% of the neonatal rats infected with 1×10^5 E44 died 48 h post-infection (Fig. 1H). In contrast, all the neonatal rats infected with 1×10^5 E44:Δ*Lpp* remained viable at the end of the observation (96 h post-infection) (Fig. 1H). The percentage of circulating white blood cells (WBC) remained unchanged in the mice infected with E44:Δ*Lpp* compared to E44 (Fig. 1I). Additional results showed that Lpp deletion have little effect on the ability of extravascular *E. coli* to enter the blood stream, and the ability of circulating *E. coli* to enter the brain through the BBB (Figs. S1A–D). These results suggested that *Lpp* contributes to the pathogenicity of *E. coli* K1 for the development of bacteremia necessary for meningitis.

2.2. Lpp-deleted E. coli is susceptible to neutrophils killing

Neutrophils are generally regarded as the first line of defense to combat the invading pathogens at the beginning of infection [5]. We thus hypothesized that the *Lpp*-deleted *E. coli* K1 may be more prone to be eliminated by neutrophils, resulting in the failure of the development of bacteremia in the meningitis model. To test this, the bone marrow-derived neutrophils (BMDNs) isolated from mice were used to evaluate the phagocytosis of the *E. coli* by neutrophils. We used bacteria uptake assay to assess the uptake of *E. coli* by BMDNs at 15 min post-infection which is at the early stage of phagocytosis, with the fluorescence of extracellular bacteria quenched. The results showed that there was no difference between the numbers of internalized E44 and E44:Δ*Lpp* within neutrophils (Fig. 2A and B). Then the isolated BMDNs were infected with the *E. coli* for 1 h to allow phagocytosis, and the viable bacteria inside the cells was determined by plating on LB agar plates, with the extracellular bacteria killed by gentamicin. We found that the viable E44:Δ*Lpp* within BMDNs was less than the viable E44 (Fig. 2C). At 1 h post-infection, the quantity of viable E44:Δ*Lpp* within BMDNs was significantly reduced to $52.46 \pm 11.56\%$ of that of E44 ($P < 0.05$, Fig. 2C). Then the polymorphonuclear neutrophils (PMNs) isolated from human peripheral blood were used to further verify the role of *Lpp* in the intracellular survival of *E. coli* K1 (Fig. 2D–F). We found that *Lpp* deletion significantly reduced the survival of the engulfed *E. coli* within PMNs, with the quantity of viable E44:Δ*Lpp* reduced to $21.04 \pm 7.66\%$ of that in E44 ($P < 0.01$, Fig. 2F). In contrast, bacteria uptake assays showed that *Lpp* deficiency had little effect on the uptake of *E. coli* by PMNs (Fig. 2D and E). Furthermore, we counted the live bacteria labeled with green fluorescent SYTO dye inside PMNs at 1 h post-infection by confocal microscopy. The results showed that the level of viable E44:Δ*Lpp* within PMNs were significantly less than that of E44 (Fig. 2G; $P < 0.01$, Fig. 2H), which is consistent with the results from gentamicin protection assays (Fig. 2F). We further found that the percentages of mature PMNs with three or more lobes were increased by infection with E44:Δ*Lpp* compared to E44 (Fig. 2I), whereas the survival of PMNs infected with E44:Δ*Lpp* was similar to that infected with E44 (Fig. 2J).

It is known that the phagocytosed bacteria are enclosed into phagosomes characterized by acidic luminal pH [5]. To test whether E44:Δ*Lpp* could withstand the acidic environment, the bacteria were exposed to the acidified media (pH 7.2, 6.5 and 5.5) containing Triton X-100 followed by the assessment of bacterial growth. The results showed that deletion of *Lpp* did not affect the sensitivity of *E. coli* K1 to the acidic environment (Fig. 2K). Another important process for the development of *E. coli* meningitis is the bacterial penetration through the blood-brain barrier, which is mainly composed of brain microvascular endothelial cells (BMEC) [21]. To test whether *Lpp* is also involved in the intracellular survival of *E. coli* K1 within BMEC, the quantity of the viable invaded *E. coli* within human BMEC was examined. No significant difference between the survived E44 and E44:Δ*Lpp* was found inside BMEC (Fig. 2L). These data indicated that deletion of *Lpp* specifically enhanced

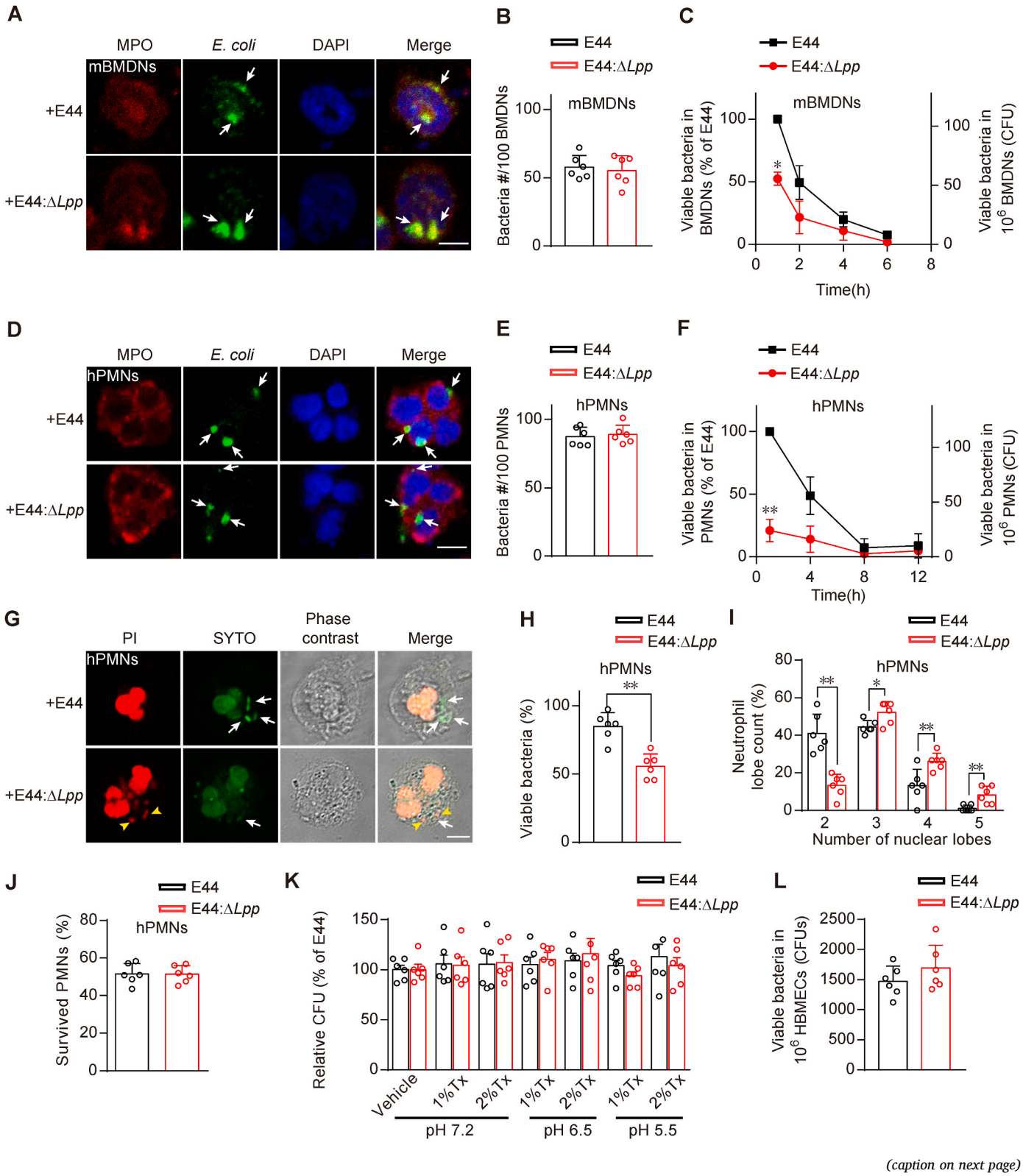

(caption on next page)

Fig. 2. Lpp-deleted *E. coli* showed reduced intracellular survival within neutrophils.
(A) The isolated murine BMDNs (mBMDNs) seeded on coverslips were infected with *E. coli* (MOI = 100) for 15 min followed by immunostaining with antibodies against *E. coli* LPS (green) and MPO (red). Typan Blue was used to quench the fluorescence of extracellular bacteria. DAPI (blue) was used for counter-staining. The slides were mounted and visualized by confocal microscope. The white arrows indicated the intracellular bacteria. Images are representative of six independent experiments. Scale bar, 5 μm. (B) Quantification of the bacteria within BMDNs from the results in (A). Data are presented as *mean* ± *SD* ($n = 6$). (C) The BMDNs were seeded to 24-well plate, then *E. coli* (MOI = 100) were added and incubated for 1 h. Gentamicin was used to kill the extracellular bacteria and the cells were cultured for indicated times. Then the cells were lysed with water and the serially diluted samples were plated on LB agar plates. The CFUs were counted following overnight culture at 37 °C. * , $P < 0.05$ ($n = 5$). (D) Similar experiments were performed as in (A) except that the BMDNs were replaced with isolated human PMNs (hPMNs). Images are representative of six independent experiments. Scale bar, 5 μm. (E) Quantification of the bacteria within PMNs from the results obtained in (D). Data are presented as *mean* ± *SD* ($n = 6$). (F) Similar experiments were performed as in (C) except that the BMDNs were replaced with isolated human PMNs. ** , $P < 0.01$ ($n = 4$). (G) The isolated PMNs were seeded on coverslips in 24-well plate and infected with *E. coli* for 1 h followed by staining with PI (red) and SYTO (green) dye. The slides were mounted and visualized by confocal microscope. The arrows indicated the intracellular live bacteria and arrowheads indicated the dead bacteria. Images are representative of six independent experiments. Scale bar, 5 μm. (H) Quantification of the live/dead bacteria within PMNs from the results obtained in (G). Data are presented as *mean* ± *SD* ($n = 6$). **, $P < 0.01$. (I) The nuclear lobs of the PMNs in G was quantified and the percentage of PMNs with 2–5 lobes were calculated and plotted. Data are presented as *mean* ± *SD* ($n = 6$). *, $P < 0.05$. **, $P < 0.01$. (J) The isolated PMNs were infected with *E. coli* (MOI = 100) for 1 h followed by typlan blue staining to identify viable cells. The percentages of the survived PMNs were calculated and plotted. Data are presented as *mean* ± *SD* ($n = 6$). (K) The overnight cultured bacteria were centrifuged and resuspended with BHI broth containing Triton X-100 with different pH. The culture were then incubated for 10 min and serially diluted to plate on LB agar plates. The CFUs were counted following incubation at 37 °C overnight. The results were presented as *mean* ± *SD* ($n = 6$). (L) The human BMEC were seeded in 24-well plate followed by the addition of the *E. coli* (MOI = 100) for 1.5-h incubation. Gentamicin was used to kill the extracellular bacteria, and then the cells were lysed with water. The serially diluted lysate were plated on LB agar plate. The CFUs were counted following overnight incubation at 37 °C. The results were presented as *mean* ± *SD* ($n = 6$). (For interpretation of the references to colour in this figure legend, the reader is referred to the Web version of this article.)

E. coli susceptibility to the intracellular bactericidal activity of neutrophils.

2.3. NETs are not involved in the clearance of Lpp-deficient E. coli by neutrophils

Release of neutrophil extracellular traps (NETs), which are composed of chromatin and neutrophil granular proteins, has been demonstrated to be a unique bactericidal strategy in neutrophils [22] except phagocytosis. As our data herein established that deletion of *E. coli Lpp* enhanced the neutrophil-mediated killing, we sought to determine whether the *Lpp*-deleted *E. coli* can enhance the release of NETs. The results from scanning electron microscopy (SEM) revealed that the extracellular web-like structures of PMNs showed no significant difference between E44 and E44:Δ*Lpp* after a 3-h incubation, with PMA (phorbol 12-myristate 13-acetate)-treated PMNs as a positive control (Fig. 3A and B). Then quantitative estimation of the extracellular DNA, representative of NETs, was performed by immunostaining using fluorescent dye SYTOX. We found that the release of extracellular DNA in neutrophils infected with E44 were similar to that of E44:Δ*Lpp* (Fig. 3C and D). In line with these results, Western blot analysis showed that H3-Cit, a citrullinated histone used as a marker of NETs, showed no difference in neutrophils infected with E44 and E44:Δ*Lpp* (Fig. 3E and F). These data demonstrated that the enhanced elimination of *Lpp*-deleted *E. coli* by neutrophils was achieved by a NETs-independent pathway.

2.4. ROS production in neutrophils is enhanced in response to Lpp-deficient E. coli

ROS are chemically reactive, oxygen-containing molecules produced as byproducts during mitochondrial electron transport. ROS represents one of the major bactericidal factors in neutrophils to destroy the engulfed bacteria [8]. To test whether the decreased intracellular survival of *Lpp*-deleted *E. coli* is related with ROS production in neutrophils, the ROS levels were monitored by flow cytometry with DHE fluorescence probe which could be dehydrogenated by the intracellular ROS showing red fluorescence. The results revealed that the ROS in PMNs showed a time-dependent increase upon *E. coli* infection (Fig. 4A). Interestingly, the ROS levels in PMNs infected with E44:Δ*Lpp* were significantly higher than those infected with E44 from 5 min to 60 min post-infection (Fig. 4A). Then we measured the ROS in PMNs infected with different MOI (multiplicity of infection) of *E. coli*, and we found the ROS production induced by E44:Δ*Lpp* was significantly enhanced compared to E44 at different bacterial loads (Fig. 4B).

To verify the alterations of ROS, H_2DCF, which could be oxidized to 2′,7′-dichlorofluorescein (DCF) in the presence of ROS, producing green fluorescence, was utilized to detect the intracellular ROS of PMNs. The results indicated that the ROS levels in PMNs upon E44:Δ*Lpp* infection were higher than those of E44, in a time- and dose-dependent manner (Fig. 4C and D). To further confirm our findings, the experiments were repeated with BMDNs and similar results were obtained showing that the ROS levels in BMDNs upon E44:Δ*Lpp* infection were higher than those of E44 (Fig. 4E and F). Next, fluorescence probes DHE and H_2DCF were used to visualize the cellular changes of ROS in PMN and BMDNs in response to *E. coli* infection, with PMA-treated cells as positive control. The results showed that E44:Δ*Lpp* infection induced higher intracellular levels of ROS than those of wild-type E44 in PMNs (Fig. 4G; $P < 0.01$, Fig. 4H; Fig. 4I; $P < 0.01$, Fig. 4J). In line with these results, the antioxidant levels, indicated by the reduced (GSH)-to-oxidized (GSSG) glutathione ratio, were reduced in PMNs infected with E44:Δ*Lpp* compared to E44 (Fig. 4K). These data demonstrated that deletion of *Lpp* in meningitic *E. coli* triggered significant ROS responses in neutrophils, resulting in the enhanced elimination of *E. coli* after bacterial phagocytosis.

2.5. Lpp-deficient E. coli activate NADPH oxidase to trigger ROS generation in neutrophils

To dissect the mechanism of ROS production induced by E44:Δ*Lpp*, the ROS levels in the *E. coli*-infected PMNs were assessed in the presence of diphenyleneiodonium (DPI), a common inhibitor of ROS production by inhibiting NADPH oxidase. We found that DPI (20 μM) effectively suppressed the ROS production induced by *E. coli* infection ($P < 0.01$, Fig. 5A). Notably, upon DPI treatment, the ROS of PMNs infected with E44:Δ*Lpp* and E44 was suppressed to similar levels (right 2 columns, Fig. 5A). Consistently, the intracellular survival of E44:Δ*Lpp* within PMNs was significantly recovered by DPI treatment ($P < 0.05$, Fig. 5B). We further found that treatment with pan-ROS scavenger N-acetyl-L-cysteine (L-NAC) was able to suppress the increase of E44:Δ*Lpp*-induced ROS production and ameliorate the decreased survival of E44:Δ*Lpp* within PMNs (Fig. 5C and D). These suggested that the increased ROS in PMNs in response to E44:Δ*Lpp* was predominantly generated by the NADPH oxidase.

NAPDH oxidase is a multi-component enzyme complex containing membrane-anchored $gp91^{phox}$ and multiple regulatory proteins including $p67^{phox}$, $p47^{phox}$, $p40^{phox}$ and the small GTPase Rac. The upregulation and membrane translocation of $p67^{phox}$ and $p47^{phox}$ is

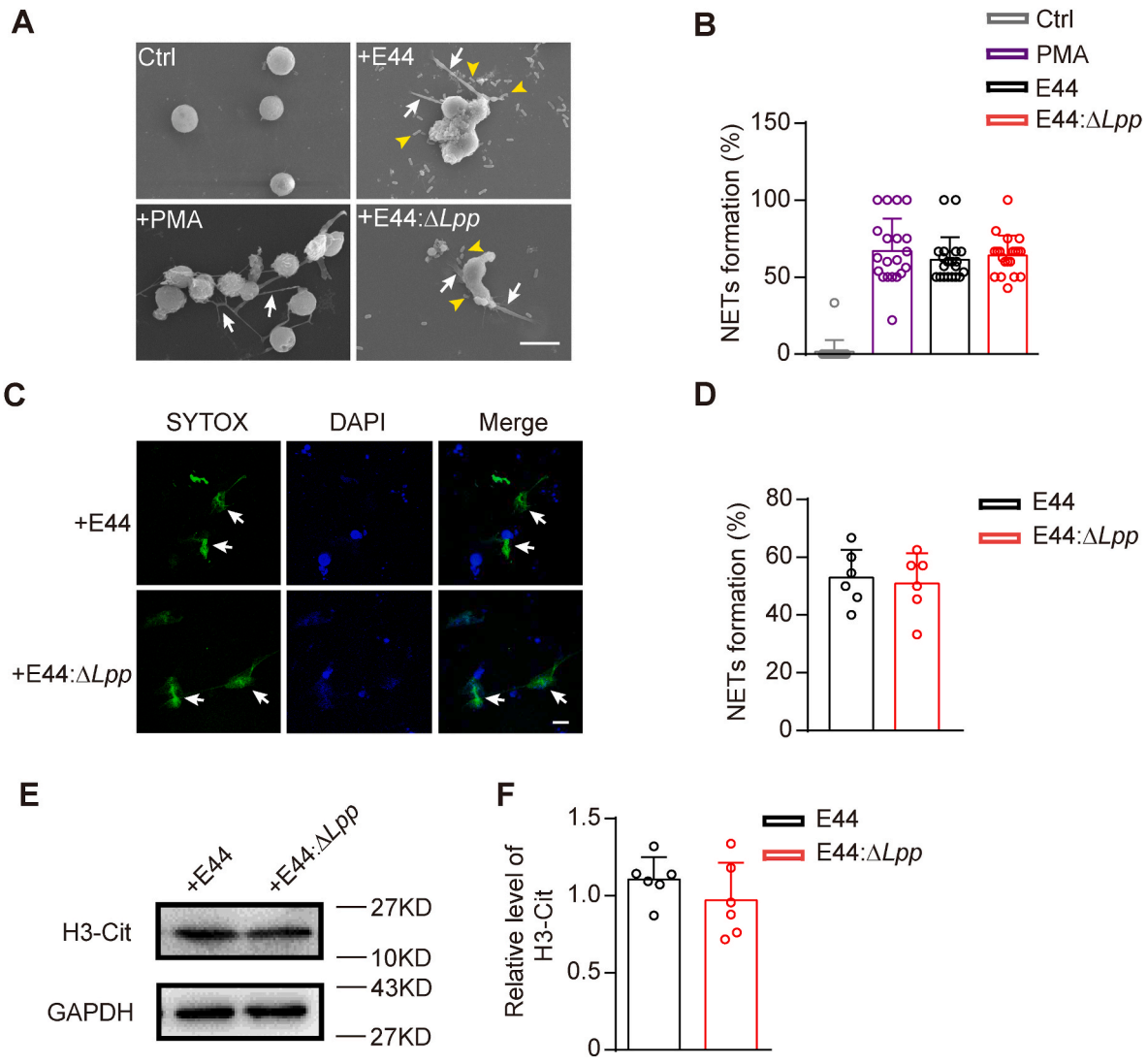

Fig. 3. The ability of *E. coli* to induce NETs was unchanged by *Lpp* deletion.
(A) The human PMNs were stimulated with *E. coli* or PMA for 3 h. Then the release of NETs was revealed by SEM. The uninfected PMNs were used as control. The arrows indicate NETs and the arrowheads indicate the extracellular bacteria. Images are representative of six independent experiments. Scale bar, 10 μm. (B) Quantification of the NETs formation by counting the percentage of PMNs with NETs under SEM in (A). For each group, more than 100 cells were counted from random fields. Data are presented as *mean* ± *SD* ($n = 20$ cells from 6 independent experiments). (C) The PMNs were seeded on coverslips and infected with *E. coli* (MOI = 100) for 3 h. The NETs were stained by SYTOX (green) with the nuclear stained with DAPI (blue) followed by imaging with confocal microscope. The arrows indicate NETs. Images are representative of six independent experiments. Scale bar, 20 μm. (D) Quantification of NETs formation by counting the percentage of PMNs with NETs revealed in the results of (C). More than 30 cells were counted from random fields for each group. Data are presented as *mean* ± *SD* ($n = 6$). (E) The PMNs were exposed to *E. coli* and the cell lysate were obtained to detect the expression of H3-Cit by Western blot, with GAPDH as loading control. Images are representative of six independent experiments. (F) The densities of the bands in western blots (E) were quantified by ImageJ software and analyzed for statistical significance. Data are presented as *mean* ± *SD* ($n = 6$). (For interpretation of the references to colour in this figure legend, the reader is referred to the Web version of this article.)

associated with the activation of NAPDH oxidase in PMNs [23]. Our Western blot analysis showed that the $p67^{phox}$ and $p47^{phox}$ levels in PMNs infected with E44:Δ*Lpp* were significantly higher than that infected with E44 (Fig. 5E). The increased $p67^{phox}$ and $p47^{phox}$ expression in PMNs infected with E44:Δ*Lpp* were attenuated by DPI treatment (Fig. 5F). Immunostaining results verified the increased cellular expression of $p67^{phox}$ and $p47^{phox}$ in PMNs infected with E44:Δ*Lpp* compared to that in E44 group (Fig. 5G), and this increase was suppressed by treatment with DPI (Fig. 5H). We further isolated the WBCs from the neonatal mice infected with *E. coli* K1 strains and the immunostaining results showed that the expression of $p47^{phox}$ in the Ly6G-expressing neutrophils challenged with E44:Δ*Lpp* were higher than that with E44 (Fig. 5I). Then we analyzed the plasma membrane translocation of $p67^{phox}$ and $p47^{phox}$, an indicator of NADPH oxidase activation [24], in the *E. coli*-infected PMNs by total internal reflection fluorescence microscopy (TIRFM). We found the puncta of $p67^{phox}$ and $p47^{phox}$ at the plasma membrane of the footprint of PMNs were significantly increased upon infection with E44:Δ*Lpp* compared to that with E44 (Fig. 5J), and this increase was attenuated by the treatment with DPI (Fig. 5K). In contrast, the expression of superoxide dismutase 1 (SOD1), glutamate-cysteine ligase catalytic subunit (GCLC), NADPH quinone acceptor oxidoreductase 1 (NQO1) and heme oxygenase 1 (HO-1), which are antioxidant proteins protecting cells from the oxidative damages caused by ROS [25], remained unchanged in PMNs treated with E44:Δ*Lpp* and E44 (Fig. 5L). The glutamate cysteine ligase modifier subunit (GCLM) expression in PMNs was reduced upon *E. coli* infection, but remained at similar levels in the PMNs infected with E44:Δ*Lpp* compared to wild-type E44 (Fig. 5L). These results collectively illustrated that *Lpp*-deleted *E. coli* upregulates $p67^{phox}$ and $p47^{phox}$ for NADPH oxidase activation to induce ROS production in neutrophils. In

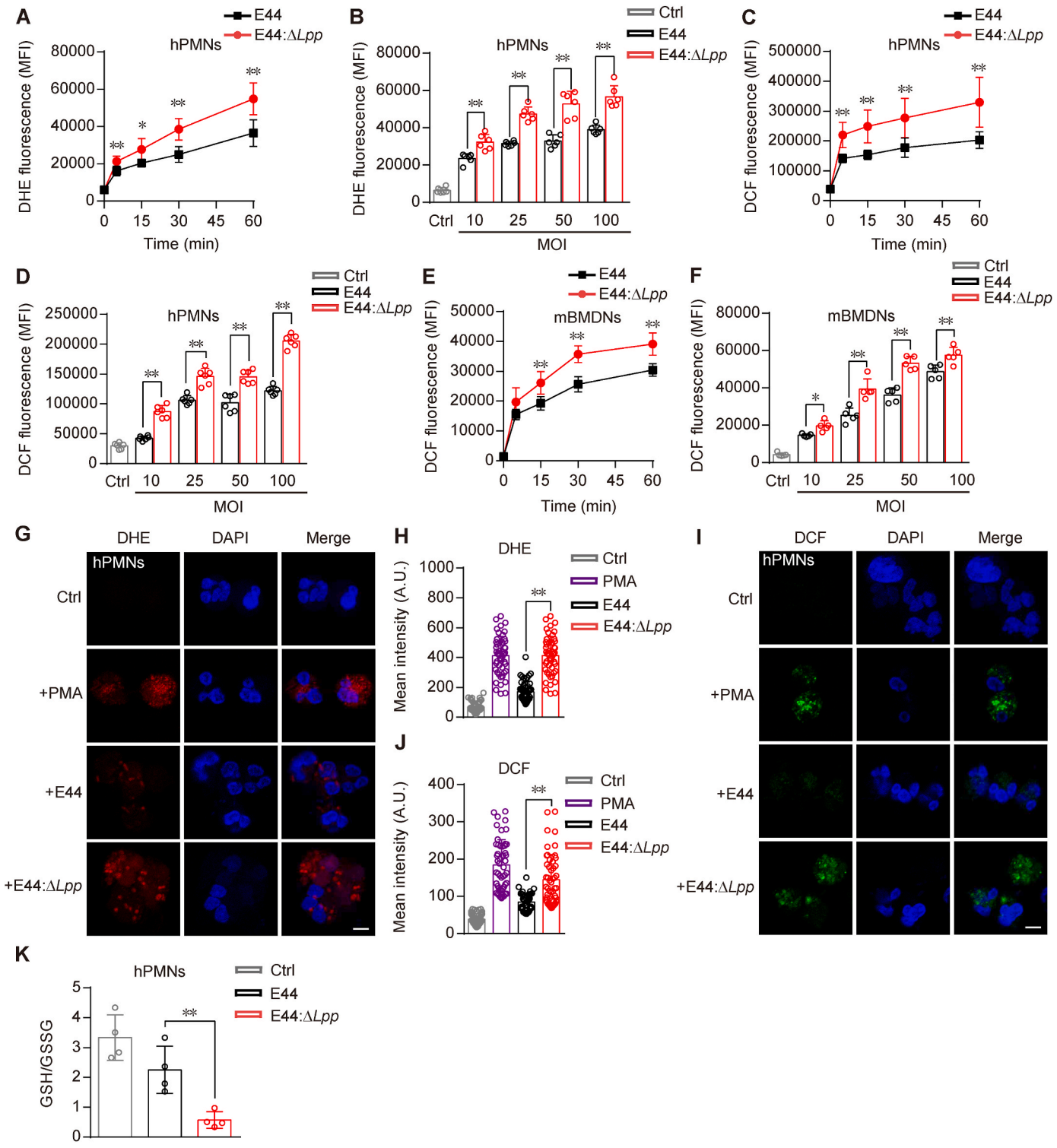

(caption on next page)

Fig. 4. ROS production was enhanced in neutrophils infected with *Lpp*-deleted *E. coli*.
(A) The isolated human PMNs were loaded with DHE dye, then the cells were infected with *E. coli* (MOI = 100) and cultured in the incubator. The cells were harvested at indicated times and the mean fluorescence intensity (MFI) was determined by flow cytometry. *, $P < 0.05$; **, $P < 0.01$ ($n = 6$). (B) The PMNs was loaded with DHE dye, then the cells were infected with *E. coli* at indicated MOI. The cells were harvested 1 h post-infection and the MFI was determined by flow cytometry. The uninfected PMNs were used as control. **, $P < 0.01$ ($n = 6$). (C, D) Similar experiments were performed as in (A) and (B), respectively, except that the ROS levels in PMNs were assessed with DCF fluorescence dye. **, $P < 0.01$ ($n = 6$). (E, F) Similar experiments were performed as in (C) and (D), respectively, except that the human PMNs were replaced with murine BMDNs from mice. *, $P < 0.05$; **, $P < 0.01$ ($n = 5$). (G) The isolated PMNs were seeded on coverslips and loaded with DHE dye (red), then the cells were infected with *E. coli* (MOI = 100) and cultured in the incubator for 1 h. The cells were then fixed and stained with DAPI (blue) for counter-staining. The slides were mounted and visualized with confocal microscope. Images are representative of six independent experiments. Scale bar, 5 μm. (H) The fluorescence intensity in the cytoplasm of PMNs infected with *E. coli* (G) were quantified. The uninfected PMNs were used as control. More than 50 cells were counted from random fields for each group. The results are from 6 independent experiments. The data are expressed as *mean* ± *SD*. **, $P < 0.01$ ($n = 50$ cells from 6 independent experiments). (I, J) Similar experiments were performed as in (G) and (H), respectively, except that the DHE dye was replaced with DCF. Scale bar, 5 μm **, $P < 0.01$ ($n = 50$ cells from 6 independent experiments). (K) The PMNs were infected with *E. coli* (MOI = 100). Then the cells were harvested 1 h post-infection and the levels of reduced glutathione (GSH) and oxidized glutathione (GSSG) were measured. The uninfected PMNs were used as control. The ratio of GSH/GSSH were calculated and plotted. **, P < 0.01 (n = 4). (For interpretation of the references to colour in this figure legend, the reader is referred to the Web version of this article.)

other words, Lpp of *E. coli* suppresses the expression and the plasma membrane translocation of $p67^{phox}$ and $p47^{phox}$ in neutrophils during infection.

2.6. Genetic ablation of host $p47^{phox}$ recovers the ability of Lpp-deleted *E. coli* to induce meningitis

To determine whether host NADPH oxidase is responsible for the Lpp-induced neutrophil activation, the *p47*^{phox} knockout mice lacking NADPH oxidase activity were established to analyze the bacterial clearance. The genetic types of the transgenic mice were identified by PCR with DNA extracted from the tails of the mice (Fig. 6A). To avoid the interference of spontaneous infection caused by the homozygous knockout of $p47^{phox}$ [26,27], the mice with heterozygous knockout of $p47^{phox}$ ($p47^{+/-}$) was used for subsequent experiments. The PMNs isolated from the peripheral blood were subjected to immunostaining and the results showed that $p47^{phox}$ expression was significantly reduced in the neutrophils of $p47^{+/-}$ mice compared to that of wild-type littermate mice ($P < 0.01$, Fig. 6B). Then the *E. coli* were injected to the neonatal $p47^{+/-}$ mice subcutaneously to induce meningitis, with wild-type littermate mice as controls. The CSF and the blood samples were collected 18 h after bacteria injection and cultured for demonstration of meningitis and bacteremia, respectively. The results showed that the levels of bacteremia evoked by E44:Δ*Lpp* strain were significantly increased in $p47^{+/-}$ mice (5.53 ± 0.72 log CFU/ml) compared with no occurrence of bacteremia in wild-type mice ($P < 0.05$, χ^2 test, Fig. 6C); while the bacteremia induced by E44 were similar in wild-type group (4.27 ± 0.89 log CFU/ml) and $p47^{+/-}$ group (4.68 ± 0.54 log CFU/ml). The incidence of meningitis induced by E44:Δ*Lpp* was increased to 25% (7/28) in the $p47^{+/-}$ mice compared with no incidence of meningitis in wild-type mice ($P < 0.05$, χ^2 test, Fig. 6C). Consistently, histological examination of the brain sections revealed the meningeal thickening and neutrophils infiltration in the meninges of the $p47^{+/-}$ mice inoculated with E44:Δ*Lpp* (Fig. 6D). These data demonstrated that genetic deficiency of host $p47^{phox}$ recovered the ability of Lpp-deleted *E. coli* to induce meningitis in neonatal mice. These results indicated that NADPH oxidase comprising $p47^{phox}$ is responsible for the elimination of ingested Lpp-deleted *E. coli*.

2.7. Lpp depletion upregulates FliC in *E. coli* to trigger ROS production in neutrophils

We found the purified recombinant Lpp protein (Fig. S2) per se did not show any inhibitory effect on the ROS levels in neutrophils (Fig. 7A). Thus we speculated that the ROS induction ability of *Lpp*-deleted *E. coli* may due to the changes of bacterial protein profiles secondary to Lpp deficiency. To test this, the differential protein profiles of E44 and E44:Δ*Lpp* were analyzed with quantitative proteomic analysis. One-way analysis of variance (ANOVA) was used to screen the differentially expressed proteins with the ratio greater than 1.2 folds. The results revealed a total number of 239 differential proteins, of which 141 were up-regulated (red spots) and 98 were down-regulated (green spots) (Fig. 7B). The gene ontology (GO) enrichment analysis of differential proteins showed that *Lpp* deletion in *E. coli* K1 caused notably changes in flagellum-related proteins (blue in Fig. 7C, Table S1).

In order to identify the particular flagellum-related proteins associated with *Lpp* deletion in *E. coli* K1, the crude flagellar proteins from E44 and E44:Δ*Lpp* were extracted and detected by SDS-PAGE followed by Coomassie brilliant blue staining (Fig. 7D). The prominent differential band of the crude flagellar proteins in E44:Δ*Lpp* were cut and identified by protein mass spectrometry. The results revealed the presence of FliC and FlgK proteins in the band (Fig. 7D), which were upregulated in E44:Δ*Lpp* (Table S1). Then we cloned the genes encoding FliC and FlgK and purified the FliC and FlgK recombinant proteins, and verified its purity by SDS-PAGE and Coomassie brilliant blue staining (Fig. 7E). The ROS production in neutrophils were then analyzed in the presence of recombinant FliC and FlgK, respectively. Interestingly, we found that the recombinant FliC can induce the generation of ROS in neutrophils in a concentration-dependent manner (Fig. 7F). In contrast, the ROS levels in neutrophils were hardly affected upon FlgK treatment (Fig. 7F). We noticed that the levels of ROS induced by recombinant FliC protein were less than that of wild-type E44 strain, suggesting the purified FliC may not function as efficiently as the endogenous FliC expressed on the bacterial flagellum. Consistently, recombinant FliC, but not FlgK, induced an increased expression of cellular $p47^{phox}$ in PMN ($P < 0.01$, Fig. 7G). Then we tested the effect of recombinant FliC on the intracellular survival of wild-type *E. coli* K1 (E44) within neutrophils. A decreased survival of E44 within PMNs was observed upon the treatment with recombinant FliC, but not with FlgK (Fig. 7H).

Furthermore, the *FliC* gene in E44:Δ*Lpp* strain was deleted using λ-Red recombination system to obtain the E44:Δ*Lpp*:Δ*FliC* strain. The deletion of *FliC* gene was verified by colony PCR (Fig. 7I). Then the ROS production in the PMNs infected with E44:Δ*Lpp*:Δ*FliC* was detected by flow cytometry using DHE fluorescence probe. We found that the ROS level evoked by E44:Δ*Lpp*:Δ*FliC* was significantly lower than that of E44:Δ*Lpp*, and was comparable to the ROS level induced by wild-type E44 (Fig. 7J), suggesting that deletion of FliC abolished the ROS-induction ability of E44:Δ*Lpp*. Then the intracellular survival of E44:Δ*Lpp*:Δ*FliC* strain within PMN was assessed by bacterial phagocytosis assay. To avoid the potential interference of bacterial adhesion impairment caused by FliC deletion [28], bacteria phagocytosis assay was performed following centrifugation to enhance the adhesion of *E. coli* to host cell surface. The results showed that deletion of *FliC* significantly recovered the reduced intracellular survival of E44:Δ*Lpp* ($P < 0.01$, Fig. 7K). The pathogenicity of E44:Δ*Lpp*:Δ*FliC* was further analyzed in the neonatal model of meningitis with 5-day-old rats. The results showed that, with the inoculation of 1×10^7 E44:Δ*Lpp*:Δ*FliC*, the quantity of *E. coli* in the blood was increased to 5.20 ± 0.93 (log

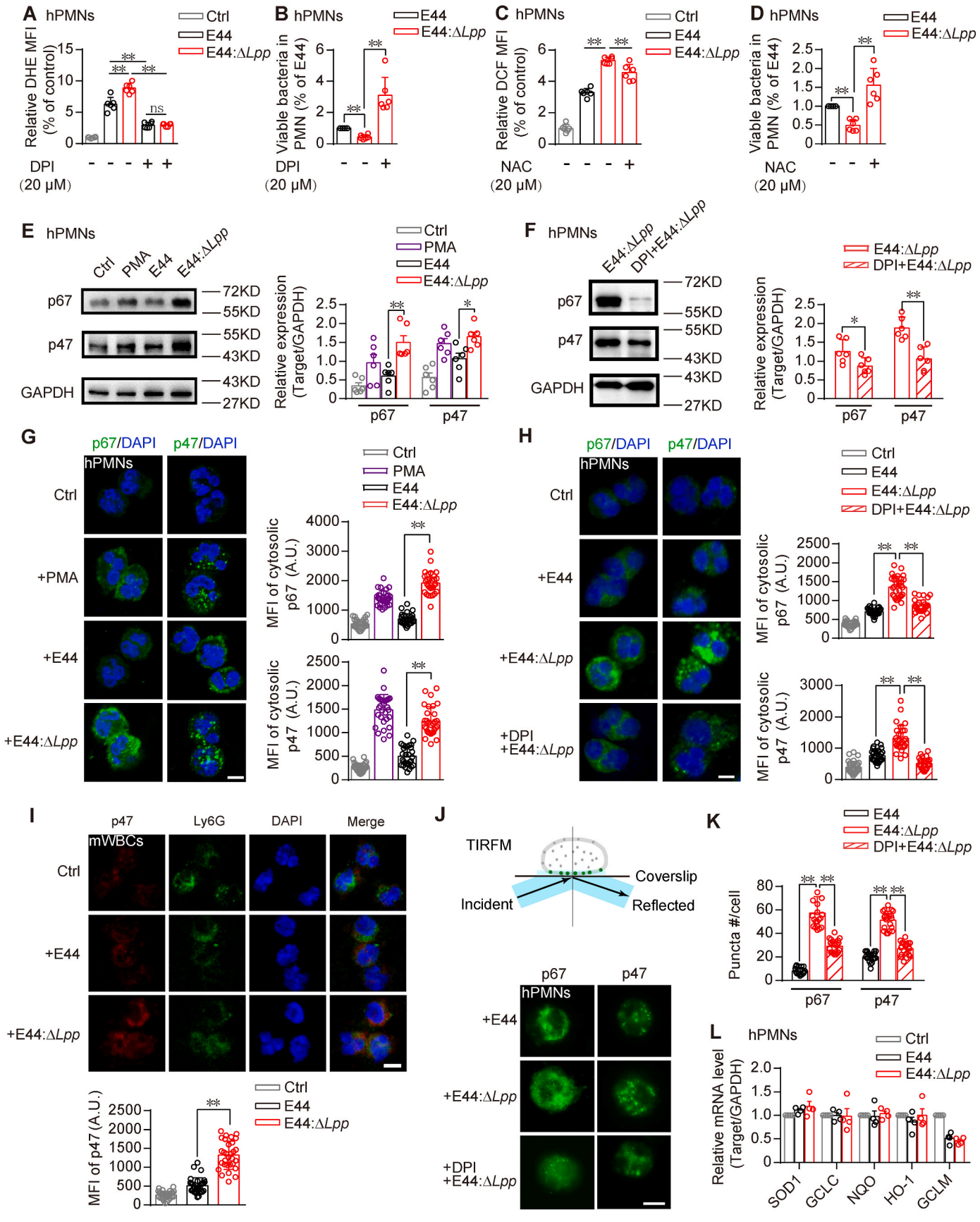

(caption on next page)

Fig. 5. *Lpp*-deleted *E. coli* activated neutrophils NADPH oxidase to produce ROS.
(A) The isolated human PMNs were loaded with DHE dye, and then the cells were pretreated with DPI (20 μM) followed by infection with *E. coli* (MOI = 100) for 1 h. The uninfected PMNs were used as control. The MFI of the cells were determined by flow cytometry. **, $P < 0.01$; ns, no significance ($n = 6$). (B) The PMNs seeded in 24-well plate were incubated in experimental medium containing DPI (20 μM). Then the *E. coli* (MOI = 100) were added and incubated for 1 h. Gentamicin was used to kill the extracellular bacteria and the cells were incubated for additional 1 h. Then the cells were lysed with water and the serially diluted samples were plated on LB agar plates. The CFUs were counted following overnight culture at 37 °C. **, $P < 0.01$ ($n = 6$). (C and D) Similar experiments were conducted except that the DPI was replaced with L-NAC and the DHE probe was replaced with DCF (C). **, $P < 0.01$ ($n = 6$). (E) The PMNs were exposed to *E. coli* or PMA for 1 h and the cell lysate were obtained to detect the expression of $p67^{phox}$ and $p47^{phox}$ by Western blot, with GAPDH as loading control. The uninfected PMNs were used as negative control (Ctrl). Images are representative of six independent experiments (left). The densities of the bands in Western blot results were quantified by ImageJ software and analyzed for statistical significance. Data are presented as *mean* ± *SD*. *, $P < 0.05$; **, $P < 0.01$ (n = 6) (right). (F) The PMNs were exposed to E44:Δ*Lpp*, in the absence or presence of DPI (20 μM), for 1 h. Then the cell lysate were obtained to detect the expression of $p67^{phox}$ and $p47^{phox}$ by Western blot, with GAPDH as loading control. Images are representative of six independent experiments (left). The densities of the bands in Western blot results were quantified by ImageJ software and analyzed for statistical significance. Data are presented as *mean* ± *SD*. *, $P < 0.05$; **, $P < 0.01$ (n = 6) (right). (G) The isolated PMNs were seeded on coverslips and infected with *E. coli* for 1 h followed by immunostaining with antibodies recognizing $p67^{phox}$ or $p47^{phox}$ (green). DAPI (blue) was used for counter-staining. The PMA-treated PMNs were used as positive control, with uninfected PMNs as negative control. The slides were visualized with confocal microscopy. Images are representative of six independent experiments. Scale bar, 5 μm (left). The mean fluorescence intensity (MFI) of the cytosolic $p67^{phox}$ or $p47^{phox}$ were quantified. At least 30 cells were counted from random fields for each group. Data are presented as *mean* ± *SD*. **, $P < 0.01$ (right). (H) The PMNs seeded on coverslips were infected with *E. coli* for 1 h followed by immunostaining with antibodies recognizing $p67^{phox}$ or $p47^{phox}$ (green). DAPI (blue) was used for counter-staining. When indicated, the cells were co-incubated with DPI (20 μM). The uninfected PMNs were used as negative control. The slides were visualized with confocal microscopy. Images are representative of six independent experiments. Scale bar, 5 μm (left). The MFI of the cytosolic $p67^{phox}$ or $p47^{phox}$ were quantified. At least 30 cells were counted from random fields for each group. Data are presented as *mean* ± *SD*. **, $P < 0.01$ (right). (I) The neonatal mice were inoculated subcutaneously with 1×10^4 *E. coli*. 18 h later, the blood were collected followed by the lysis of red blood cells. The remaining WBCs were then diluted and plated on the coverslips for immunostaining with Ly6G antibody (green) and $p47^{phox}$ antibody (red). DAPI (blue) was used for counter-staining. The WBCs from uninfected neonatal mice were used as negative control. The slides were visualized with confocal microscopy. Images are representative of six independent experiments. Scale bar, 5 μm (top). The MFI of the cytosolic $p47^{phox}$ were quantified. At least 30 cells were counted from random fields for each group. Data are presented as *mean* ± *SD*. **, $P < 0.01$ (bottom). (J and K) Schematic diagram depicting the TIRF microscopy (TIRFM) for imaging the membrane localized proteins (top panel, J). The isolated human PMNs seeded on coverslips were infected with *E. coli* for 1 h followed by immunostaining with $p67^{phox}$ and $p47^{phox}$ antibody, respectively. When indicated, the cells were co-incubated with DPI (20 μM). The footprint of the cells were visualized by TIRFM. Images are representative of six independent experiments. Scale bar, 5 μm (bottom panel, J). The puncta of $p67^{phox}$ and $p47^{phox}$ visualized at the plasma membrane footprint of PMNs in were quantified. At least 20 cells were counted from random fields for each group. Data are presented as *mean* ± *SD*. **, $P < 0.01$ (K). (L) The human PMNs were infected with *E. coli* (MOI = 100) for 1 h and the total RNA were extracted, with uninfected PMNs as control. Reverse transcription was performed and the mRNA levels of the target genes were examined by real-time quantitative PCR. Data are normalized to the control and presented as *mean* ± *SD* ($n = 4$). (For interpretation of the references to colour in this figure legend, the reader is referred to the Web version of this article.)

CFU/ml), causing a 50% incidence of meningitis (Fig. 1E). The levels of bacteremia and the meningitis incidence rate were significantly higher than that inoculated with 1×10^7 E44:Δ*Lpp* (Fig. 1E), indicating FliC deletion significantly recovered the pathogenicity of E44:Δ*Lpp*. These results demonstrated that bacterial flagellar protein FliC is responsible for the ROS production in neutrophils caused by *Lpp*-deficient *E. coli* K1.

3. Discussion

Evasion of *E. coli* K1 from the surveillance of host immune system is essential for the development of *E. coli* bacteremia and meningitis. In this study, we demonstrated the novel role of Lpp, a bacterial lipoprotein, in *E. coli* resistance to neutrophil killing. We found that *E. coli* Lpp is dedicated to restrain the expression and membrane translocation of $p67^{phox}$ and $p47^{phox}$, major components of the NADPH oxidase, to inhibit the ROS generation which is necessary for the bactericidal activity of neutrophils (Fig. 7L). We thus identified Lpp as an important bacterial factor to facilitate the intracellular survival of phagocytosed *E. coli* K1 within neutrophils.

Bacterial penetration through the BBB is thought to be one of the major step during the development of *E. coli* K1 meningitis. A number of bacterial virulence factors participating the bacterial penetration through the BBB have been characterized in *E. coli* K1, including outer-membrane protein A (OmpA), type 1 fimbriae (FimH), cytotoxic necrotizing factor 1 (CNF1), Ibe proteins [21]. Besides crossing the BBB, the interplay between *E. coli* and host immune cells is critical to the occurrence of meningitis, but the underlying mechanism remained incompletely understood. To our knowledge, Lpp is the first identified *E. coli* K1 factor specifically associated with bacterial survival within neutrophils without affecting the bacterial internalization. OmpA has been reported to be involved in bacterial survival within phagocytic cells [29,30], yet the association of OmpA with diverse processes like bacterial invasion [31] and adhesion [32] to brain endothelial cells, and the binding of OmpA with gp96 receptor on host cell surface [33] collectively indicated that OmpA may be not particularly associated with the intracellular survival of *E. coli*. The *E. coli* Lpp-dependent pathway thus represents a unique mechanism protecting the intracellular *E. coli* from the attacking of neutrophils.

The intracellular ROS is the major mediator responsible for the bactericidal activity of neutrophils. Bacterial pathogens are able to induce ROS generation in neutrophils and the induction mechanism was attributed to the bacteria-derived lipopolysaccharide (LPS), N-formylmethionine-leucyl-phenylalanine (fMLP), etc [23]. While host neutrophils have developed effective ROS-dependent attacking pathways, bacterial pathogens evolve a number of strategies to counteract the ROS generation mechanism in neutrophils. So far, whether and how *E. coli* can resist the ROS-mediated elimination remained poorly understood. Here we present a novel mechanism by which *E. coli* K1 regulate ROS production in neutrophils. The *E. coli* lipoprotein Lpp exhibits the ability to suppress the generation of ROS (Fig. 4) to enhance the survival of *E. coli* K1 within neutrophils (Fig. 2). It was reported that bacterial pathogens usually utilize toxins and effectors, such as the lethal toxins of *Bacillus anthracis* [34], the ExoS effector of *Pseudomonas aeruginosa* [13], etc., to restrain the host signal transduction pathways mediating oxidative burst in neutrophils. Distinct from these toxins and effectors, the ROS inhibitory effect of Lpp is achieved by suppressing the expression of flagellar protein FliC (Fig. 7B–D) which is shown to be able to trigger ROS generation in neutrophils (Fig. 7F–J).

FliC, also known as flagellin, constitutes the flagellar filament of bacteria and is present in several bacterial strains like *E. coli*, *Salmonella enterica* and *Pseudomonas aeruginosa*, etc [35]. FliC is found to be involved in bacterial motility [36], biofilm formation [37], type 2 secretion [38]. The experimental evidence regarding the function of *E. coli* K1 FliC was very few, and the only available study reported that FliC is involved in *E. coli* K1 adhesion with and invasion into brain microvascular endothelial cells [39]. The study of FliC in other *E. coli* strains suggested that FliC may induce chemokine expressions in colonic epithelial cells [40] and cause liver injuries in mice [41]. Here we

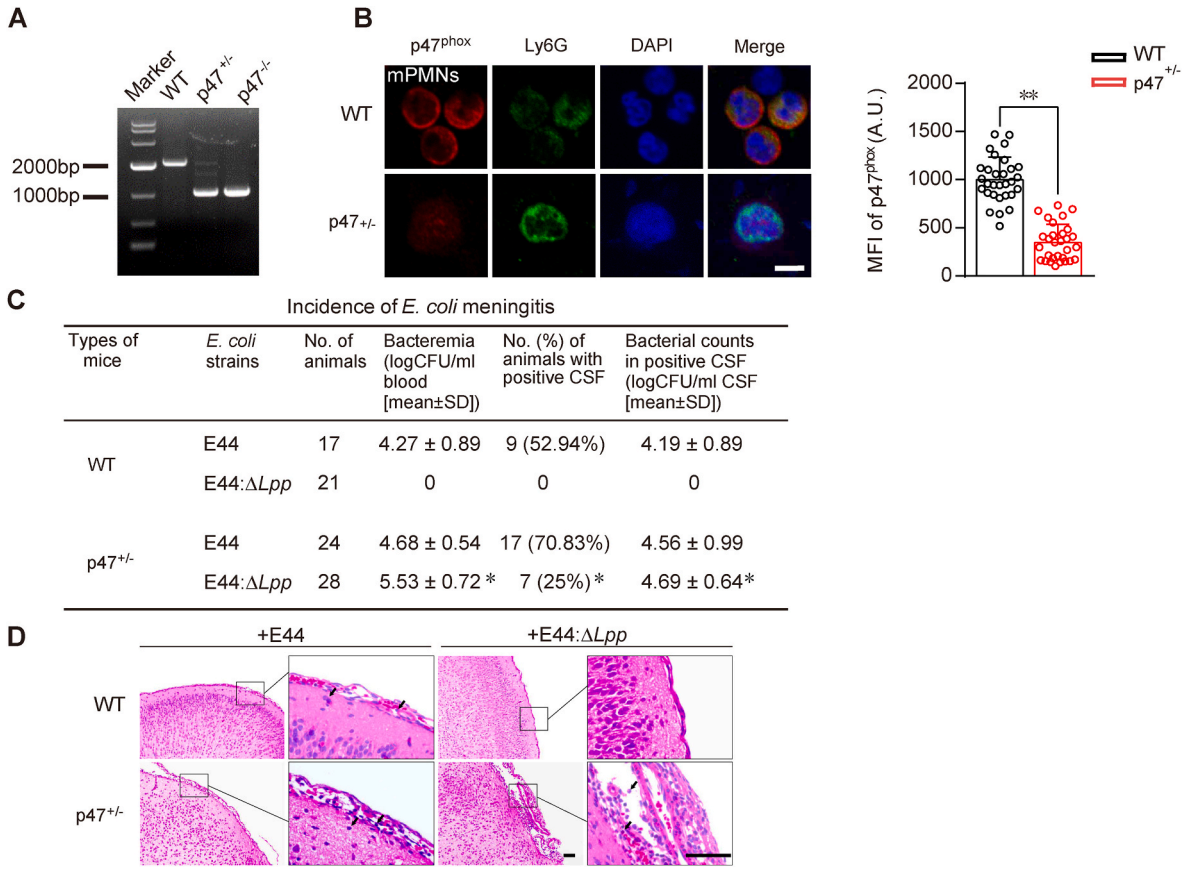

C

Incidence of *E. coli* meningitis

Types of mice	*E. coli* strains	No. of animals	Bacteremia (logCFU/ml blood [mean±SD])	No. (%) of animals with positive CSF	Bacterial counts in positive CSF (logCFU/ml CSF [mean±SD])
WT	E44	17	4.27 ± 0.89	9 (52.94%)	4.19 ± 0.89
	E44:Δ*Lpp*	21	0	0	0
$p47^{+/-}$	E44	24	4.68 ± 0.54	17 (70.83%)	4.56 ± 0.99
	E44:Δ*Lpp*	28	5.53 ± 0.72 *	7 (25%) *	4.69 ± 0.64*

Fig. 6. The reduced occurrence of meningitis in neonatal mice upon E44:Δ*Lpp* infection was recovered by *p47*^{phox} knockout.
(A) Genomic DNA was extracted from mouse tails for genotyping PCR and the products were analyzed by agarose gel electrophoresis. (B) The murine PMNs were isolated and seeded on the coverslips followed by immunostaining with antibodies recognizing Ly6G and p47^{phox}, respectively. DAPI was used for counter-staining. The slides were then visualized with confocal microscopy. Images are representative of six independent experiments. Scale bar, 5 μm (left). The MFI of p47^{phox} from at least 30 cells from random fields for each group was measured and plotted. **, $P < 0.01$ ($n = 6$) (right). (C) The 5-day-old neonatal mice were inoculated with 10^4 CFUs *E. coli* subcutaneously. The blood and CSF were collected 18 h post-infection to assess the bacteremia and the occurrence of meningitis, respectively. The rate of meningitis occurrence was calculated by dividing the number of mice with positive CSF culture by the total number of mice. The results were expressed as *mean* ± *SD*. *, $P < 0.05$ (χ^2 test). (D) The brain sections of neonatal mice inoculated with *E. coli* 18 h post-infection were prepared for H&E staining. The zoom-in view showing the meningeal thickening and neutrophils infiltration (arrows) were provided. Scale, 100 μm. The images are representative of six independent experiments.

identified the novel role of *E. coli* FliC in ROS induction in neutrophils supported by the evidence that 1) deletion of *FliC* gene attenuated the capability of *E. coli* to induce ROS in neutrophils (Figs. 7J), and 2) recombinant FliC protein is able to enhance ROS generation in neutrophils in a dose-dependent manner (Fig. 7F). FliC can bind with Toll like receptor 5, an important family member of pattern recognition receptors, to activate the proinflammatory transcription factor NF-κB, leading to activation of innate immune responses [42,43]. Here we characterize the ability of FliC to trigger ROS production within neutrophils for microbial killing activity. Our findings extend the understanding of FliC from inflammatory response induction to host defense mechanism. Given the presence of FliC across diverse bacterial species, whether the FliC-induced ROS generation represents a general mechanism to trigger the respiratory burst in neutrophils is an interesting issue to be determined.

Neutrophil extracellular traps (NETs), composed of nuclear DNA associated with histones and granule proteins, are recognized as an important strategy to trap and destroy the invading pathogens [22]. A number of studies indicate that formation of NETs is a ROS-dependent process [44]. Here we found that the NETs remained unaltered (Fig. 3) whereas the intracellular ROS level was increased (Fig. 4) in the neutrophils infected with *Lpp*-deleted *E. coli*, suggesting that NETs formation is not necessarily dependent on the ROS levels. It is known that excess ROS may produce oxidative stress causing harmful effects, including DNA damages, NETs formation, cell death or even cell lysis [45]. In our study, the NETs remained unaffected in neutrophils infected with Lpp-deleted *E. coli* (Fig. 3), we thus proposed that the ROS was increased to a moderate but not excessive level in the neutrophils challenged with Lpp-deleted *E. coli*. Our findings are in line with recent reports revealing the ROS-independent NETs in neutrophils exposed to lipopolysaccharide or soluble immune complexes [46,47]. Our work thus adds to the emerging evidence that endogenous ROS are not strictly required for NETs formation, though they can contribute to this process in certain situations.

It has been shown that the translocation of p47^{phox} and p67^{phox} to the plasma membrane was caused by the structural modifications induced by their phosphorylation [48]. Multiple kinases, including protein kinase C, protein kinase A, Akt, ERK, and p38 mitogen-activated protein kinase were reported to be the enzyme responsible for the phosphorylation of p47^{phox} and p67^{phox} [48]. Whether and how Lpp-deleted E44 exploit these kinases to regulate phosphorylation of p47^{phox} and p67^{phox} for their membrane translocation is an interesting issue to be determined in the future study.

We found the level of FliC is increased upon deletion of *Lpp* in *E. coli* K1, suggesting Lpp could inhibit the expression of FliC under physiological condition. This raised the issue that how Lpp regulate the expression of FliC in *E. coli* K1. A recent study showed that NlpE, an outer membrane lipoprotein of enterohemorrhagic *E. coli*, activates Cpx

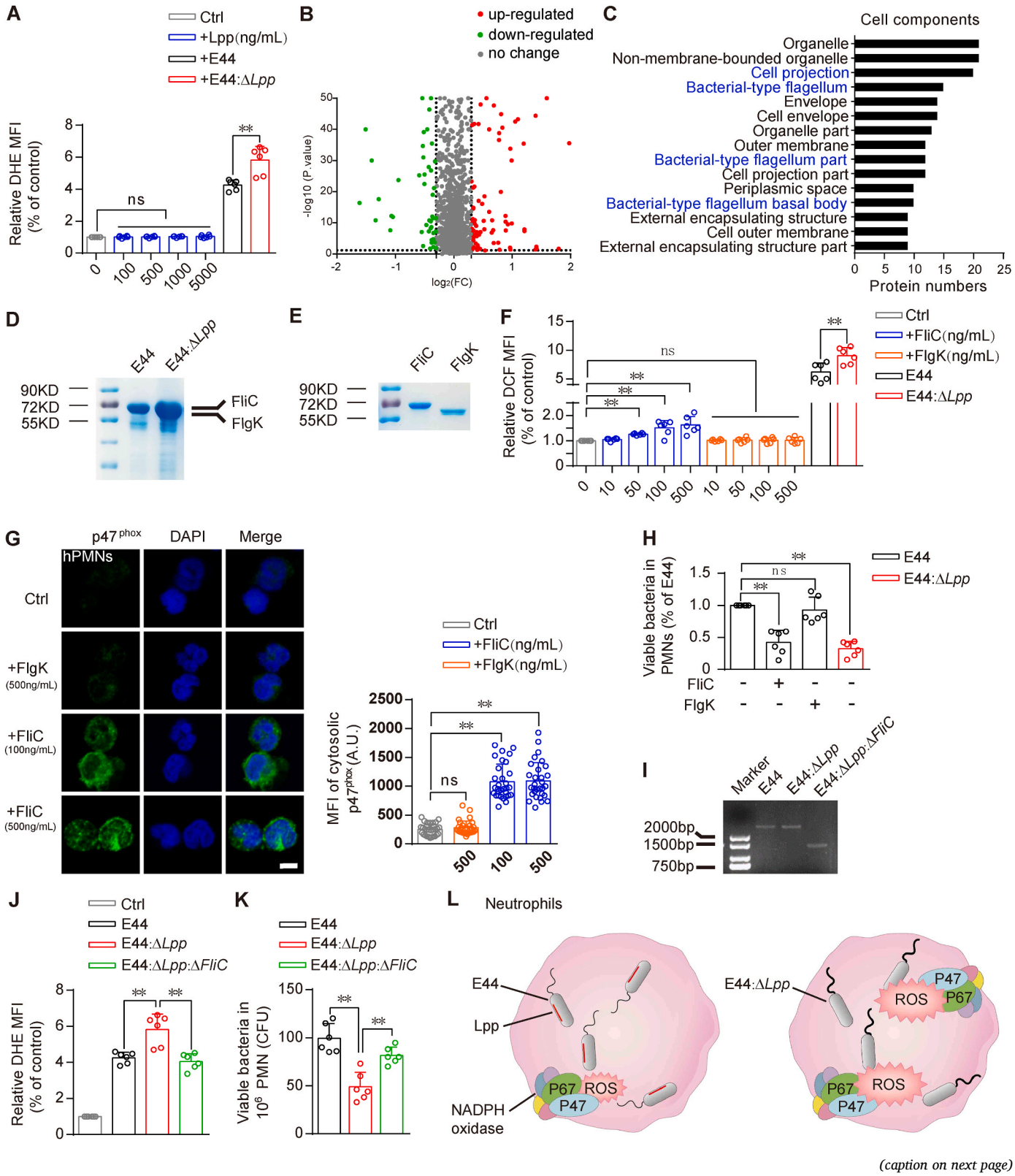

(caption on next page)

Fig. 7. *Lpp* depletion upregulates FliC in *E. coli* to trigger ROS production in neutrophils
(A) The isolated human PMNs were loaded with DCF dye followed by the treatment with recombinant Lpp proteins at indicated concentrations for 1 h. For comparison, the PMNs loaded with DCF were treated with *E. coli* (MOI = 100) for 1 h. The mean fluorescence intensity (MFI) of DCF was detected by flow cytometry. The results were expressed as *mean* ± *SD*. *, $P < 0.05$ ($n = 6$). (B) The overnight culture of *E. coli* were collected for proteomic analysis. The differential protein between E44 and E44:Δ*Lpp* was presented as volcano diagram. (C) Gene ontology enrichment analysis of the differentially expressed protein between E44 and E44:Δ*Lpp*. (D) The overnight culture of *E. coli* were collected, then the crude bacterial flagellum protein were extracted and analyzed by SDS-PAGE followed by Coomassie brilliant blue staining. The prominent band were subjected to mass spectrometry analysis and the identified proteins were labeled. (E) The cDNA of *FliC* and *FlgK* gene were amplified from E44 strain and cloned into pET28a(+) vector for *in vitro* protein expression and purification. The purified FliC and FlgK proteins were analyzed by SDS-PAGE followed by Coomassie brilliant blue staining. (F) The isolated PMNs were loaded with DCF dye followed by the treatment with FliC and FlgK proteins at indicated concentrations for 1 h. For comparison, the PMNs loaded with DCF were treated with E44 or E44:Δ*Lpp* (MOI = 100) for 1 h. The fluorescence of DCF was detected by flow cytometry. The results were expressed as *mean* ± *SD*. **, $P < 0.01$ ($n = 6$). (G) The isolated human PMNs were seeded on coverslips and treated with recombinant proteins for 1 h followed by immunostaining with $p47^{phox}$ antibody (green). DAPI (blue) was used for counter-staining. The slides were visualized with confocal microscopy. Images are representative of six independent experiments. Scale bar, 5 μm (left panel). The MFI of the cytosolic $p47^{phox}$ were quantified. At least 30 cells from random fields were quantified for each group. Data are presented as *mean* ± *SD*. **, $P < 0.01$ ($n = 6$) (right panel). (H) The PMNs infected with E44 were pretreated with recombinant FliC or FlgK and incubated for 1 h, then gentamicin was added to kill the extracellular bacteria. For comparison, the PMNs were infected with E44:Δ*Lpp* for 1 h. The cell lysate were diluted and plated on LB agar plates. The bacterial CFUs were counted after culture at 37 °C overnight. The results were presented as *mean* ± *SD*. **, $P < 0.01$ ($n = 6$); (I) The *FliC* gene in E44:Δ*Lpp* strain was removed by homologous recombination and the mutant strain with deletion of both *Lpp* and *FliC* (E44:Δ*Lpp*:Δ*FliC*) was identified by colony PCR followed by gel electrophoresis. The parent strains E44 and E44:Δ*Lpp* were used as controls. (J) The PMNs were loaded with DHE dye followed by the addition of the indicated *E. coli* strains (MOI = 100). After incubation for 1 h, the fluorescence of the cells were detected by flow cytometry. The results were presented as *mean* ± *SD*. **, $P < 0.01$ ($n = 6$). (K) The isolated human PMNs were infected with indicated *E. coli* for 1 h, then gentamicin was added to kill the extracellular bacteria. The cell lysate were diluted and plated on LB agar plates. The bacterial CFUs were counted after culture at 37 °C overnight. The results were presented as *mean* ± *SD*. **, $P < 0.01$ ($n = 6$). (L) Schematic illustrating the role of *E. coli* Lpp in ROS production of neutrophils. (For interpretation of the references to colour in this figure legend, the reader is referred to the Web version of this article.)

signal transduction pathway to inhibit the expression of flagella proteins via the transcriptional regulator LysR homologue A (LrhA) [49]. It will be interesting to investigate whether bacterial Lpp utilizes the similar pathway to restrain the expression of FliC in *E. coli* K1.

In summary, we identified the novel role of *E. coli* lipoprotein Lpp in bacterial resistance to neutrophil killing by suppressing host ROS production. *E. coli* Lpp is able to inhibit the expression of flagella protein FliC to downregulate host NADPH oxidase, resulting in diminished oxidative burst and impaired bactericidal activity in neutrophils.

4. Material and methods

4.1. Ethics statement

The research use of peripheral blood from the healthy volunteers was approved by the Institutional Review Board of the First Hospital of China Medical University (2020-2020-237-2). Enrolled 82 volunteers were adults younger than 50 years without any infectious disease and fever. All study participants were provided informed written consent prior to study enrollment. The studies were performed following the guidelines of the World Medical Association's Declaration of Helsinki.

The $p47^{phox}$ knockout mice (C57BL/6JSmoc-*Ncf1*^{em1Smoc}, Cat# NM-KO-190123) were obtained from Shanghai Model Organisms Center (Shanghai, China). This mouse line was established by deletion of the exon 3 and exon 4 of $p47^{phox}$ encoding gene *Ncf1* using CRISPR-Cas9 technology. The animals used in this study were raised in Department of Laboratory Animal Center of China Medical University and the animal experiments were approved by the Institutional Animal Care and Use Committees (IACUC) by China Medical University (IACUC# CMU2020076, CMU2021213).

4.2. Bacterial strains

E. coli K1 RS218 (O18: K1: H7) was isolated from cerebrospinal fluid of patients with neonatal meningitis [50], and E44 was a rifampin resistant mutant. The bacteria were cultured in BHI (Brain Heart Infusion) broth (BD Biosciences, Sparks, MD) containing 100 μg/mL rifampin at 37 °C overnight.

4.3. Construction of isogenic deletion mutant strain

The *Lpp* gene in E44 strain of meningitis *E. coli* was knocked out by λ-Red recombination system. A DNA fragment was amplified from plasmid pKD13 containing the resistant gene and flanking sequences of *Lpp* gene with primers (forward: 5′- CGCTACATGGAGATTAACTCAATCTAGAGGGTATTAATAGTGTAGGCTGGAGCTGCTTCG-3′; reverse: 5′- GGCGCACATCGTGCGCCATTTTTCACTTCACAGGTACTAATTCCGGGGATCCGTCGACC-3′). Then the fragment was transformed into E44 strain containing pLP6 plasmid to replace the *Lpp* gene. The resistant gene was then removed by plasmid pCP20 with flippase enzyme, resulting in the E44:Δ*Lpp* strain.

The *FliC* gene in E44:Δ*Lpp* strain was knocked out using λ-Red recombination system. The upstream and downstream homologous DNA fragments of the *FliC* gene were amplified from E44:Δ*Lpp* strain with primers (forward: 5′-GGAATCTAGACCTTGAGTCGTTGGCGGTCTGGAAAGTTGT-3′; reverse: 5′-ACAGCTAGCGACGATATGTCCCTTGTAGGGCGTCATAGCGT-3′; forward: 5′- CGTCTGTCTTCTGGCTTGCGTATGCGACCGAAGTGTCCAAC-3′; reverse: 5′- ACAGCTAGCGACGATATGTCCCTTGTAGGGCGTCATAGCGT-3′) respectively and linked up by overlap extension PCR. Then the fragment was transformed into E44:Δ*Lpp* strain by plasmid plP12 resulting in the E44:Δ*Lpp*:Δ*FliC* strain.

4.4. Growth curve analysis

The bacteria were inoculated to LB broth containing rifampicin (100 μg/ml) at a ratio of 1:100 and cultured at 37 °C, 225 rpm. OD 600 nm was determined at indicated times by spectrophotometer and the bacterial growth curve was plotted.

4.5. Bacterial sensitivity analysis

To test the bacterial sensitivity to the detergent, the bacteria strains were cultured to an OD 600 nm of 0.4–0.5, and then transferred to the medium containing Triton X-100 at indicated concentrations at a ratio of 1:50. OD 600 nm was measured after further incubation for 3 h at 37 °C, 225 rpm. A 50% reduction in the OD value indicated a breach in the bacterial membrane integrity.

For the bacterial sensitivity to pH, the overnight bacterial culture were centrifuged and the pellets were resuspended in BHI broth with different pH (7.2, 6.5 or 5.5) and Triton X-100 (0, 1 or 2%). After a 10-min treatment at room temperature, the samples were serially diluted followed by plating on LB agar plates containing rifampin, and cultured at 37 °C overnight. The bacterial survival rates were calculated as the percentages of viable bacteria relative to the control groups.

4.6. Neonatal meningitis model of rodents

The Sprague Dawley rats were randomly grouped according to weight at 5 days of age without gender selection, and the 1×10^5 (or as indicated) CFU *E. coli* K1 were subcutaneously injected to each rats as describe previously [51]. The rats were sacrificed 18 h post-injection to collect the cerebrospinal fluid and blood. The collected samples (2-μl volume) were then serially diluted and enumerated by plating on LB agar plates containing rifampin followed by culturing at 37 °C overnight. The number of CFU was counted next morning.

For survival analysis, the rats were subcutaneously injected with 1×10^5 CFU of the *E. coli*, and the survival curves were plotted according to the Kaplan–Meier method.

For mice, the 5-day-old neonatal mice were randomly grouped without gender selection and injected with 1×10^4 CFU *E. coli* K1 subcutaneously. Then the cerebrospinal fluid and blood samples were collected for analysis at 18 h post infection.

4.7. Isolation of human PMNs

Peripheral blood was drawn from volunteers and anti-coagulated by EDTA. Red blood cells were removed by red blood cell lysis buffer followed by centrifugation. PMNs were separated using Ficoll-Paque Plus (GE healthcare) and resuspended in RPMI1640 containing 5% fetal bovine serum. Cell viability and purity was assessed by Trypan blue and flow cytometry, respectively.

4.8. Isolation of mouse BMDNs

The bone marrow derived neutrophils (BMDNs) were isolated from the femur and tibia of 8-week-old male C57/BL6 mice. The bone marrow cavity was rinsed with pre-cooled RPMI1640 medium and collected for centrifugation. The supernatant was discarded and the red blood cells were removed by red blood cell lysis buffer followed by centrifugation. Percoll separation solution with discontinuous density gradient (81%, 62%, 55%, from bottom to top) was added. The re-suspended cells were slowly added to the surface of the separation liquid. After centrifugation at 2000 rpm for 30 min, cells between 62% and 81% of the separation layer were obtained and washed with PBS. The obtained cells were then resuspended in RPMI1640 medium containing 5% FBS.

4.9. Cell culture

Human BMEC (brain microvascular endothelial cells) were cultured in RPMI1640 medium containing 10% fetal bovine serum (Gibco), 10% Nu-serum (BD Biosciences), 2 mM glutamine, 1 mM sodium pyruvate, 1 x nonessential amino acid, and 1 x minimal essential medium (MEM) vitamin. Cells were incubated at 37 °C in a 5% CO_2, 100% humidified incubator.

4.10. Bacterial invasion/phagocytosis assay

The intracellular survival of *E. coli* K1 within human BMEC or PMNs was evaluated as described previously [51]. Briefly, cells were seeded into 24-well plates with 1×10^6 cells/well. The bacteria were added at a multiplicity of infection (MOI) of 100 (1×10^7 CFU/well). The plates were incubated at 37 °C for 1 h to allow invasion to occur. The viable invaded bacteria inside BMEC or the phagocytosed bacteria within PMNs were determined by live/dead bacteria staining and gentamicin protection assay.

For the live/dead bacteria staining, the PMNs were resuspended with staining buffer (0.1 M MOPS, 1 mM $MgCl_2$, 0.1% saponin) containing fluorescence dye SYTO (60 μM) and propidium iodide (10 μM) that label live and dead bacteria, respectively, and incubated at room temperature for 15 min. The intracellular live bacteria were counted under confocal laser scanning microscope (Nikon A1R).

For the gentamicin protection assay, the number of intracellular bacteria was determined after the extracellular bacteria were killed by incubation with experimental medium containing gentamicin (100 μg/ml) for 1 h at 37 °C. The cells were then washed twice with RPMI1640 and lysed with 200 μl deionized water. Serial dilution was prepared and 20 μl of diluted lysate were enumerated by plating on LB agar plates containing rifampin and cultured at 37 °C overnight. For quantifications, the viable bacteria were counted by CFUs.

4.11. Immunofluorescence

The cells were fixed with 4% paraformaldehyde and permeabilized with 0.2% Triton X-100 and then blocked with 5% bovine serum albumin (BSA) in PBS. Then the cells were stained with antibody against MPO, LPS, $p67^{phox}$ or $p47^{phox}$ or Ly6G (1:200 dilution) and then incubated with secondary antibody conjugated with Alexa488 or Alexa555 (1:200 dilution, Invitrogen), respectively. For the analysis of NETs formation, the isolated PMNs (1×10^6) were seeded on coverslips coated with poly-L-lysine, and incubated with *E. coli* (MOI = 100) or treated with PMA (100 ng/mL) for 3 h at 37 °C followed by staining with SYTOX Green (Invitrogen) for 15 min before fixation. Following DAPI staining, the coverslips were mounted and analyzed under confocal microscope (Nikon A1R).

4.12. Bacteria uptake assay

The PMNs or BMDNs seeded on coverslips were infected with *E. coli* (MOI = 100) for 15 min. Then the cells were fixed for immunostaining with antibodies against *E. coli* and the cells. Typan Blue was used to quench the fluorescence of the extracellular *E. coli*. DAPI was used for counter-staining. The slides were mounted and the intracellular bacteria per cell were identified and counted by confocal microscopy.

4.13. TIRF microscopy

Isolated PMNs (1×10^6) were seeded on poly-L-lysine coated coverslips, followed by the bacteria invasion (MOI = 100) for 1 h at 37 °C. The cells were then fixed with 4% paraformaldehyde and permeabilized with 0.2% Triton X-100. After blocking with 5% BSA, the cells were stained with antibody against $p67^{phox}$ or $p47^{phox}$ (1:200 dilution) and incubated with secondary antibody conjugated with Alexa488 (1:200 dilution, Invitrogen). The images of the cell membrane were collected with a TIRF microscope (Olympus), using UPLAPO 100X objective (1.5 N A.). The puncta on the cell membrane were measured and quantified for statistical analysis.

4.14. Flow cytometry

Isolated PMNs (1×10^6) were incubated at 37 °C for 30 min with DHE (5 nM, MedChemExpress, USA) or H_2DCFDA (5 nM, MedChemExpress). Subsequently, the cells were incubated with bacteria or purified flagellar protein for 1 h at 37 °C. Cells were washed and resuspended in PBS, and subjected to analysis with flow cytometer (Accuri C6 Plus, BD Biosciences).

4.15. GSH/GSSG assay

Human PMNs were infected with different *E. coli* strains. Then the cells were added to the wells of a 96-well luminometer-compatible plate followed by measurement with GSH/GSSG-Glo Assay Kit (Promega, V6612) according to manufacturer's instructions. In brief, the Total Glutathione Lysis Reagent were added to the wells for the measurement of total glutathione levels, and the Oxidized Glutathione Lysis Reagent were added to the parallel wells for the measurement of the levels of oxidized glutathione (GSSG). Then the Luciferin Generation Reagent and Luciferin Detection Reagent was added to the wells followed by the

measurement of the luminescence with microplate reader. The levels of reduced glutathione (GSH) was determined by removing the values of GSSG from the total glutathione. Then the ratio of GSH/GSSG were calculated for quantifications.

4.16. Scanning electron microscopy

Isolated PMNs (1×10^6) were seeded on coverslips and incubated for 1 h at 37 °C. Then the cells were treated with PMA (100 ng/ml) or infected with bacteria (MOI = 100) for 3 h, followed by washing with cold PBS. Cells were fixed with 2.5% glutaraldehyde solution (Sigma-Aldrich) and washed 3 times with PBS at 4 °C. The cells were postfixed in 1% osmium tetroxide and centrifuged with density-gradient ethanol and butanol for 10 min for dehydration. After freeze-drying, the PMNs were visualized and recorded by a scanning electron microscope (Hitachi SU3500, Japan).

4.17. Western blot

Cells were washed with ice-cold PBS and lysed with RIPA buffer (50 mM Tris–HCl, 150 mM NaCl, 1% NP-40, 0.5% sodium deoxycholate, 0.1% sodium dodecyl sulfate) containing protease inhibitor cocktail. The samples were separated by SDS-PAGE and then transferred to polyvinylidene difluoride (PVDF) membrane (Millipore). The PVDF membrane was blocked with 5% nonfat milk and incubated with antibody against H3-Cit (1:1000 dilution, Abcam), $p67^{phox}$ (1:1000 dilution, Abcam), $p47^{phox}$ (1:1000 dilution, Gene Tex) at 4 °C overnight. Then the blots were incubated with an HRP-conjugated secondary antibody (1:5000 dilution, Santa Cruz Biotech) for 1 h at room temperature. Immunoreactive bands were visualized by Super Signal West Pico chemiluminescent substrate (Thermo Fisher) using Tanon-5200 chemiluminescent imaging system (Tanon, China).

4.18. Quantitative RT-PCR

The total RNA isolated with TRIzol reagent (Invitrogen) was reverse transcribed using HiScript II Q Select RT SuperMix (Vazyme Biotech). ChamQ Universal SYBR qPCR Master Mix (Vazyme Biotech) was used for quantitative PCR on 7500 Real-Time PCR System (Applied Biosystem). The relative gene expressions were calculated by comparative CT method. Samples were examined in triplicate. The following primers were used: human SOD1 (forward: 5′- GGAAGTCGTTTGGCTTGTGG-3′; reverse: 5′- GGGCCTCAGACTACATCCAAG-3′), human NQO1 (forward: 5′- TTGGAGTCCCTGCCATTCTGA-3′; reverse: 5′- CTGCCTTCTTAC TCCGGAAGG-3′), human GCLC (forward: 5′- CGGAGGAA-CAATGTCCGAGT-3′; reverse: 5′- AAGGTACTGAAGCGAGGGTG-3′), human HO-1 (forward: 5′-TGTGGCAGCTGTCTCAAACCTCCA-3′; reverse: 5′-TTGAGGCTGAGCCAGGAACAGAGT-3′), human GCLM (forward: 5′-ACAGGTAAAACCAAATAGTAACCAAGTTAA-3′; reverse: 5′-TGTTTAGCAAATGCAGTCAAATCTG-3′), human GAPDH (forward: 5′-AAGGTGAAGGTCGGAGTCAAC-3′; reverse: 5′-GGGGTCATTGATGG-CAACAATA-3′).

4.19. Extraction of crude flagellar proteins

The bacterial strains were cultured overnight and collected by centrifugation at 4 °C, 5000 g for 15 min. The pellets were resuspended with 20 mM Tris-HCl (pH 8.0) and stirred on magnetic stirrer for 90 s, then the supernatant were obtained by centrifugation and crude flagellar proteins in the supernatant were extracted through salt precipitation and adequate dialysis. The crude flagellar proteins were examined by SDS-PAGE followed by Coomassie bright blue staining.

4.20. Purification of recombinant FliC and FlgK protein

The *fliC* and *flgK* gene were amplified from E44 strain by PCR and inserted into the pET28a(+) vector, respectively, then the constructs were transformed into *E. coli* strain BL21. The expression was induced by IPTG (isopropyl β-D-1-thiogalactopyranoside) and the supernatant of bacterial lysate was purified by metal ion affinity chromatography. Samples were eluted with buffer containing 250 mM imidazole, and then the buffer was exchange to PBS through a Sephadex-G25 chromatographic column. Then the eluted fraction was polished by gel filtration and the purified protein was analyzed with SDS-PAGE followed by Coomassie blue staining.

4.21. Proteomics analysis

The *E. coli* were cultured overnight and the proteins were extracted and quantified. The proteins were digested into peptide by trypsin which were marked by isotope and pre-dissociated by strong cation exchange column. The purified components were eluted using a gradient of 5–80% (v/v) acetonitrile in 0.1% formic acid over 45 min at a flow rate of 300 nL/min combined with a Q Exactive mass spectrometer (Thermo Fisher Scientific, MA, USA). The Proteome Discoverer 1.4 software (Thermo Fisher Scientific) was used for screening and the spectrogram was scanned using mascot. Significant difference was evaluated by ANOVA, and the proteins with $P < 0.05$, ratio$\leq$0.83 or $\geq$1.2 were considered as differential proteins.

4.22. Statistical analysis

The data were analyzed by Graphpad Prism 9 software. Each experiment was repeated at least six times. Statistical significance between two groups was analyzed by Student's *t*-test. ANOVA was used to compare multiple groups. Differences were considered significant when $P < 0.05$.

Declaration of competing interest

The authors declare the following financial interests/personal relationships which may be considered as potential competing interests: Wei-Dong Zhao reports financial support was provided by National Natural Science Foundation of China. Wei-Dong Zhao reports financial support was provided by Liaoning Province Government.

Data availability

No data was used for the research described in the article.

Acknowledgments

We would like to acknowledge the helpful comments on our manuscript from the late Dr. Kwang Sik Kim. This work was supported by the National Natural Science Foundation of China (31870832, 81901915, 32000811), the Program of Distinguished Professor of Liaoning Province (LJH2018-35) and the Innovation Team Project of Liaoning Province Colleges (LJH2020-386).

Appendix A. Supplementary data

Supplementary data to this article can be found online at https://doi.org/10.1016/j.redox.2022.102588.

References

[1] W. El-Naggar, J. Afifi, D. McMillan, J. Toye, J. Ting, E.W. Yoon, et al., Epidemiology of meningitis in Canadian neonatal intensive care units, Pediatr. Infect. Dis. J. 38 (5) (2019) 476–480.
[2] C. Woll, M.I. Neuman, C.M. Pruitt, M.E. Wang, E.D. Shapiro, S.S. Shah, et al., Epidemiology and etiology of invasive bacterial infection in infants </=60 Days old treated in emergency departments, J. Pediatr. 200 (2018), 210-217 e1.

[3] M. Xu, L. Hu, H. Huang, L. Wang, J. Tan, Y. Zhang, et al., Etiology and clinical features of full-term neonatal bacterial meningitis: a multicenter retrospective cohort study, Front Pediatr 7 (2019) 31.

[4] L. Snoek, B.P. Gonçalves, E. Horváth-Puhó, M.N. van Kassel, S.R. Procter, K. K. Søgaard, et al., Short-term and long-term risk of mortality and neurodevelopmental impairments after bacterial meningitis during infancy in children in Denmark and the Netherlands: a nationwide matched cohort study, Lancet Child Adolesc Health 6 (9) (2022) 633–642.

[5] W.M. Nauseef, N. Borregaard, Neutrophils at work, Nat. Immunol. 15 (7) (2014) 602–611.

[6] A. Furuta, A. Brokaw, G. Manuel, M. Dacanay, L. Marcell, R. Seepersaud, et al., Bacterial and host determinants of group B streptococcal infection of the neonate and infant, Front. Microbiol. 13 (2022), 820365.

[7] B. Shahan, E.Y. Choi, G. Nieves, Cerebrospinal fluid analysis, Am. Fam. Physician 103 (7) (2021) 422–428.

[8] C.C. Winterbourn, A.J. Kettle, M.B. Hampton, Reactive oxygen species and neutrophil function, Annu. Rev. Biochem. 85 (2016) 765–792.

[9] Herre M, Cedervall J, Mackman N, Olsson AK. Neutrophil extracellular traps in the pathology of cancer and other inflammatory diseases. Physiol. Rev.. 2023;103(1): 277-312.

[10] C.N. Paiva, M.T. Bozza, Are reactive oxygen species always detrimental to pathogens? Antioxidants Redox Signal. 20 (6) (2014) 1000–1037.

[11] K. Chandra, A. Roy Chowdhury, R. Chatterjee, D. Chakravortty, GH18 family glycoside hydrolase Chitinase A of Salmonella enhances virulence by facilitating invasion and modulating host immune responses, PLoS Pathog. 18 (4) (2022), e1010407.

[12] G.Y. Lam, R. Fattouh, A.M. Muise, S. Grinstein, D.E. Higgins, J.H. Brumell, Listeriolysin O suppresses phospholipase C-mediated activation of the microbicidal NADPH oxidase to promote Listeria monocytogenes infection, Cell Host Microbe 10 (6) (2011) 627–634.

[13] C. Vareechon, S.E. Zmina, M. Karmakar, E. Pearlman, A. Rietsch, Pseudomonas aeruginosa effector ExoS inhibits ROS production in human neutrophils, Cell Host Microbe 21 (5) (2017) 611–618 e5.

[14] A.T. Asmar, J.F. Collet, Lpp, the Braun lipoprotein, turns 50-major achievements and remaining issues, FEMS Microbiol. Lett. 365 (18) (2018).

[15] E.J. Cohen, J.L. Ferreira, M.S. Ladinsky, M. Beeby, K.T. Hughes, Nanoscale-length control of the flagellar driveshaft requires hitting the tethered outer membrane, Science 356 (6334) (2017) 197–200.

[16] A.T. Asmar, J.L. Ferreira, E.J. Cohen, S.H. Cho, M. Beeby, K.T. Hughes, et al., Communication across the bacterial cell envelope depends on the size of the periplasm, PLoS Biol. 15 (12) (2017), e2004303.

[17] J. Sha, A.A. Fadl, G.R. Klimpel, D.W. Niesel, V.L. Popov, A.K. Chopra, The two murein lipoproteins of Salmonella enterica serovar typhimurium contribute to the virulence of the organism, Infect. Immun. 72 (7) (2004) 3987–4003.

[18] P.L. Fisette, S. Ram, J.M. Andersen, W. Guo, R.R. Ingalls, The Lip lipoprotein from Neisseria gonorrhoeae stimulates cytokine release and NF-kappaB activation in epithelial cells in a Toll-like receptor 2-dependent manner, J. Biol. Chem. 278 (47) (2003) 46252–46260.

[19] T. Liu, S.L. Agar, J. Sha, A.K. Chopra, Deletion of Braun lipoprotein gene (lpp) attenuates Yersinia pestis KIM/D27 strain: role of Lpp in modulating host immune response, NF-kappaB activation and cell death, Microb. Pathog. 48 (1) (2010) 42–52.

[20] K.S. Doran, M. Fulde, N. Gratz, B.J. Kim, R. Nau, N. Prasadarao, et al., Host-pathogen interactions in bacterial meningitis, Acta Neuropathol. 131 (2) (2016) 185–209.

[21] K.S. Kim, Current concepts on the pathogenesis of Escherichia coli meningitis: implications for therapy and prevention, Curr. Opin. Infect. Dis. 25 (3) (2012) 273–278.

[22] O.E. Sorensen, N. Borregaard, Neutrophil extracellular traps - the dark side of neutrophils, J. Clin. Invest. 126 (5) (2016) 1612–1620.

[23] G.T. Nguyen, E.R. Green, J. Mecsas, Neutrophils to the ROScue: mechanisms of NADPH oxidase activation and bacterial resistance, Front. Cell. Infect. Microbiol. 7 (2017) 373.

[24] R. Rastogi, X. Geng, F. Li, Y. Ding, NOX activation by subunit interaction and underlying mechanisms in disease, Front. Cell. Neurosci. 10 (2016) 301.

[25] E.T. de Lemos, J. Oliveira, J.P. Pinheiro, F. Reis, Regular physical exercise as a strategy to improve antioxidant and anti-inflammatory status: benefits in type 2 diabetes mellitus, 2012, Oxid. Med. Cell. Longev. (2012), 741545.

[26] S.H. Jackson, J.I. Gallin, S.M. Holland, The p47phox mouse knock-out model of chronic granulomatous disease, J. Exp. Med. 182 (3) (1995) 751–758.

[27] A. Pizzolla, M. Hultqvist, B. Nilson, M.J. Grimm, T. Eneljung, I.M. Jonsson, et al., Reactive oxygen species produced by the NADPH oxidase 2 complex in monocytes protect mice from bacterial infections, J. Immunol. 188 (10) (2012) 5003–5011.

[28] Q. Duan, M. Zhou, X. Zhu, Y. Yang, J. Zhu, W. Bao, et al., Flagella from F18+ Escherichia coli play a role in adhesion to pig epithelial cell lines, Microb. Pathog. 55 (2013) 32–38.

[29] R. Mittal, N.V. Prasadarao, gp96 expression in neutrophils is critical for the onset of Escherichia coli K1 (RS218) meningitis, Nat. Commun. 2 (2011) 552.

[30] S.K. Sukumaran, H. Shimada, N.V. Prasadarao, Entry and intracellular replication of Escherichia coli K1 in macrophages require expression of outer membrane protein A, Infect. Immun. 71 (10) (2003) 5951–5961.

[31] R. Maruvada, K.S. Kim, IbeA and OmpA of Escherichia coli K1 exploit Rac1 activation for invasion of human brain microvascular endothelial cells, Infect. Immun. 80 (6) (2012) 2035–2041.

[32] C.H. Teng, Y. Xie, S. Shin, F. Di Cello, M. Paul-Satyaseela, M. Cai, et al., Effects of ompA deletion on expression of type 1 fimbriae in Escherichia coli K1 strain RS218 and on the association of E. coli with human brain microvascular endothelial cells, Infect. Immun. 74 (10) (2006) 5609–5616.

[33] R. Maruvada, Y. Argon, N.V. Prasadarao, Escherichia coli interaction with human brain microvascular endothelial cells induces signal transducer and activator of transcription 3 association with the C-terminal domain of Ec-gp96, the outer membrane protein A receptor for invasion, Cell Microbiol. 10 (11) (2008) 2326–2338.

[34] M.A. Crawford, C.V. Aylott, R.W. Bourdeau, G.M. Bokoch, Bacillus anthracis toxins inhibit human neutrophil NADPH oxidase activity, J. Immunol. 176 (12) (2006) 7557–7565.

[35] M. Nedeljkovic, D.E. Sastre, E.J. Sundberg, Bacterial flagellar filament: a supramolecular multifunctional nanostructure, Int. J. Mol. Sci. 22 (14) (2021).

[36] K.D. Smith, E. Andersen-Nissen, F. Hayashi, K. Strobe, M.A. Bergman, S.L. R. Barrett, et al., Toll-like receptor 5 recognizes a conserved site on flagellin required for protofilament formation and bacterial motility, Nat. Immunol. 4 (12) (2003) 1247–1253.

[37] M. Zhou, Z. Guo, Y. Yang, Q. Duan, Q. Zhang, F. Yao, et al., Flagellin and F4 fimbriae have opposite effects on biofilm formation and quorum sensing in F4ac+ enterotoxigenic Escherichia coli, Vet. Microbiol. 168 (1) (2014) 148–153.

[38] T. Suriyanarayanan, S. Periasamy, M.H. Lin, Y. Ishihama, S. Swarup, Flagellin FliC phosphorylation affects type 2 protease secretion and biofilm dispersal in Pseudomonas aeruginosa PAO1, PLoS One 11 (10) (2016), e0164155.

[39] G. Parthasarathy, Y. Yao, K.S. Kim, Flagella promote Escherichia coli K1 association with and invasion of human brain microvascular endothelial cells, Infect. Immun. 75 (6) (2007) 2937–2945.

[40] T.J. Rogers, A.W. Paton, S.R. McColl, J.C. Paton, Enhanced CXC chemokine responses of human colonic epithelial cells to locus of enterocyte effacement-negative shiga-toxigenic Escherichia coli, Infect. Immun. 71 (10) (2003) 5623–5632.

[41] Y. Xiao, F. Liu, J. Yang, M. Zhong, E. Zhang, Y. Li, et al., Over-activation of TLR5 signaling by high-dose flagellin induces liver injury in mice, Cell. Mol. Immunol. 12 (6) (2015) 729–742.

[42] A.T. Gewirtz, T.A. Navas, S. Lyons, P.J. Godowski, J.L. Madara, Cutting edge: bacterial flagellin activates basolaterally expressed TLR5 to induce epithelial proinflammatory gene expression, J. Immunol. 167 (4) (2001) 1882–1885.

[43] F. Hayashi, K.D. Smith, A. Ozinsky, T.R. Hawn, E.C. Yi, D.R. Goodlett, et al., The innate immune response to bacterial flagellin is mediated by Toll-like receptor 5, Nature 410 (6832) (2001) 1099–1103.

[44] C. Dahlgren, A. Karlsson, J. Bylund, Intracellular neutrophil oxidants: from laboratory curiosity to clinical reality, J. Immunol. 202 (11) (2019) 3127–3134.

[45] B. Amulic, C. Cazalet, G.L. Hayes, K.D. Metzler, A. Zychlinsky, Neutrophil function: from mechanisms to disease, Annu. Rev. Immunol. 30 (2012) 459–489.

[46] K. Chen, H. Nishi, R. Travers, N. Tsuboi, K. Martinod, D.D. Wagner, et al., Endocytosis of soluble immune complexes leads to their clearance by FcgammaRIIIB but induces neutrophil extracellular traps via FcgammaRIIA in vivo, Blood 120 (22) (2012) 4421–4431.

[47] E. Pieterse, N. Rother, C. Yanginlar, L.B. Hilbrands, J. van der Vlag, Neutrophils discriminate between lipopolysaccharides of different bacterial sources and selectively release neutrophil extracellular traps, Front. Immunol. 7 (2016) 484.

[48] M. Mittal, M.R. Siddiqui, K. Tran, S.P. Reddy, A.B. Malik, Reactive oxygen species in inflammation and tissue injury, Antioxidants Redox Signal. 20 (7) (2014) 1126–1167.

[49] T. Shimizu, K. Ichimura, M. Noda, The surface sensor NlpE of enterohemorrhagic Escherichia coli contributes to regulation of the type III secretion system and flagella by the Cpx response to adhesion, Infect. Immun. 84 (2) (2016) 537–549.

[50] S.H. Huang, Y.H. Chen, Q. Fu, M. Stins, Y. Wang, C. Wass, et al., Identification and characterization of an Escherichia coli invasion gene locus, ibeB, required for penetration of brain microvascular endothelial cells, Infect. Immun. 67 (5) (1999) 2103–2109.

[51] W.D. Zhao, D.X. Liu, J.Y. Wei, Z.W. Miao, K. Zhang, Z.K. Su, et al., Caspr1 is a host receptor for meningitis-causing Escherichia coli, Nat. Commun. 9 (1) (2018) 2296.